A Multi-Stage Joint Planning and Operation Model for Energy Hubs considering Integrated Demand Response Programs

S. A. Mansouri [1*], A. Ahmarinejad [2], F. Sheidaei[1], M. S. Javadi [3], A. Rezaee Jordehi[4], A. Esmaeel Nezhad [5] and J. P. S. Catalão[3,6]

[1] Department of Electrical Engineering, Yadegar-e-Imam Khomeini (RAH) Shahre Rey Branch, Islamic Azad University, Tehran, Iran
[2] Department of Electrical Engineering, Central Tehran Branch, Islamic Azad University, Tehran, Iran
[3] Institute for Systems and Computer Engineering, Technology and Science (INESC TEC), Porto, Portugal
[4] Department of Electrical Engineering, Rasht Branch, Islamic Azad University, Rasht, Iran
[5] Department of Electrical Engineering, School of Energy Systems, LUT University, 53850, Lappeenranta, Finland
[6] Faculty of Engineering of the University of Porto, Porto, Portugal

Abstract

Energy hub systems improve energy efficiency and reduce emissions due to the coordinated operation of different infrastructures. Given that these systems meet the needs of customers for different energies, their optimal design and operation is one of the main challenges in the field of energy supply. Hence, this paper presents a two-stage stochastic model for the integrated design and operation of an energy hub in the presence of electrical and thermal energy storage systems. As the electrical, heating, and cooling loads, besides the wind turbine's (WT's) output power, are associated with severe uncertainties, their impacts are addressed in the proposed model. Besides, demand response (DR) and integrated demand response (IDR) programs have been incorporated in the model. Furthermore, the real-coded genetic algorithm (RCGA), and binary-coded genetic algorithm (BCGA) are deployed to tackle the problem through continuous and discrete methods, respectively. The simulation results show that considering the uncertainties leads to the installation of larger capacities for assets and thus a 8.07% increase in investment cost. The results also indicate that the implementation of shiftable IDR program modifies the demand curve of electrical, cooling

[*] Corresponding Author: Amir.mansouri24@gmail.com

and heating loads, thereby reducing operating cost by 15.1%. Finally, the results substantiate that storage systems with discharge during peak hours not only increase system flexibility but also reduce operating cost.

Keywords: Energy Hub Planning; Genetic Algorithm; Integrated Demand Response Programs; Wind Turbine; Energy Storage Systems; Stochastic Programming.

Nomenclature

Acronyms	
WT	Wind Turbine
DR	Demand Response
IDR	Integrated Demand Response
RCGA	Real-Code Genetic Algorithm
BCGA	Binary-Code Genetic Algorithm
EES	Electrical Energy Storage
TES	Thermal Energy Storage
CHP	Combined Heat and Power
PV	Photovoltaic
MT	Microturbine
EH	Electrical Heater
EHP	Electric Heat Pomp
AC	Absorption Chiller
DER	Distributed Energy Resource
RER	Renewable Energy Resource
EV	Electric Vehicle
MCS	Monte Carlo Simulation
MILP	Mixed-Integer Linear Programming
MINLP	Mixed-Integer Nonlinear Programming
Sets	
t	Index of time slots (h)
ω	Index of seasons
γ	Index of scenarios
k	Index of demand response programs
em	Index of emissions
Scalars	
$ELF(\gamma,\omega)$	Equivalent loss factor
η_{ee}^{T}	Efficiency factor of the transformer
η_{ee}^{Con}	Efficiency factor of the ac/ac converter
η_{eh}^{EHP}	Efficiency factor of the EHP
η_{ec}^{EHP}	Efficiency factor of the EHP

η_{ge}^{CHP}	Electrical efficiency factor of the CHP unit
η_{gh}^{CHP}	Heating efficiency factor of the CHP unit
η_{gh}^{B}	Efficiency factor of the Boiler
η_{eh}^{EH}	Efficiency factor of the heater
$\eta_{EES/TES}^{ch}$	ESS/TES system's charging efficiency
$\eta_{EES/TES}^{dis}$	ESS/TES system's discharging efficiency
LPF^{shup}	Load participation factor for shift up DR
LPF^{shdo}	Load participation factor for shift down DR
$\alpha_{EES/TES}^{Initial}$	The energy, available in the EES/TES system at the beginning of scheduling (kWh)
$\alpha_{EES/TES}^{Final}$	The energy, available in the EES/TES system at the end of scheduling (kWh)
$\alpha_{EES/TES}^{Loss}$	Loss factor of EES / TES
$\alpha_{EES/TES}^{min,ch}$	Minimum charging factor relating to the EES/TES system
$\alpha_{EES/TES}^{max,ch}$	Maximum charging factor relating to the EES/TES system
EF_{em}^{CHP}	Emission coefficient of the CHP
EF_{em}^{B}	Emission coefficient of the Boiler
v_{ci}	Cut-in speed of the WT (km/h)
v_{co}	Cut-out speed of the WT (km/h)
v_r	Rated speed of the WT (km/h)
Parameters	
$P_{ec}^{Install}(c)$	Installation candidates of each asset (kW)
$\rho(sc)$	The probability associated with each scenario of load demand
$\varphi(\omega)$	The number of days of each season
$\pi_e^{Net,Buy}(\omega,t)$	The cost, imposed to the system due to transacting power with the utility grid (\$/kWh)
$\pi_e^{Net,Sell}(\omega,t)$	The revenue, obtained by exporting power to the utility grid (\$/kWh)
π_g^{Net}	The price of natural gas (\$/kWh)
π_e^{W}	The cost due to wind power generation (\$/kWh)
π_e^{ENS}	The ENS cost (\$/kWh)
π_{em}	The cost imposed due to emissions (\$/kg)
π_e^{S}	The operating of the EES system (\$/kWh)
π_h^{S}	The operating cost of the TES (\$/kWh)
IC_{ec}	Investment cost, relating to the assets (\$/kW)
$P_e(\gamma,\omega,t)$	Power demand before applying the DR (kW)
$v(\gamma,\omega,t)$	Wind speed (km/h)
Variables	
TC^{Hub}	Total cost of hub (\$/year)
IC^{Hub}	Investment cost of hub (\$/year)
OC^{Hub}	Operating cost of hub (\$/year)
C_{ec}	Installed capacity for each asset (kW)

P_{ec}^{max}	Maximum capacity of each asset (kW)
$P_e^{Net,Buy}(\gamma,\omega,t)$	The amount of power imported from the utility grid (kW)
$P_e^{Net,Sell}(\gamma,\omega,t)$	The amount of power exported to the utility grid (kW)
$P_e^{W}(\gamma,\omega,t)$	Power generated by the wind turbine (kW)
$P_g^{Net,CHP}(\gamma,\omega,t)$	The amount of gas consumed by the CHP unit (kW)
$P_g^{Net,B}(\gamma,\omega,t)$	The amount of gas consumed by the boiler (kW)
$P_e^{ch}(\gamma,\omega,t)$	Charging power of the EES system (kW)
$P_e^{dis}(\gamma,\omega,t)$	Discharging power of the EES system (kW)
$P_h^{ch}(\gamma,\omega,t)$	Charging power of the TES (kW)
$P_h^{dis}(\gamma,\omega,t)$	Discharging power of the TES (kW)
P_e^{ENS}	Energy not served (kW)
$P_g^{Net}(\gamma,\omega,t)$	Imported natural gas (kW)
$E_{EES/TES}^{S}(\gamma,\omega,t)$	Energy stored in EES/TES (kWh)
$E_{EES/TES}^{Loss}$	Losses of EES/TES system (kW)
$P_{EES/TES}^{dis}$	Discharging power of the ESS/TES system (kW)
$P_{e,h,c}^{+}(\gamma,\omega,t)$	Shifted-up load by DR (kW)
$P_{e,h,c}^{-}(\gamma,\omega,t)$	Shifted-down load by DR (kW)
$P_h^{EHP}(\gamma,\omega,t)$	Heating generation of EHP (kW)
$P_c^{EHP}(\gamma,\omega,t)$	Cooling power generation by the EHP (kW)
P_e^{EH}	The amount of power consumed by the heater (kW)
$P_h^{AC}(\gamma,\omega,t)$	Heat consumed by absorption chiller (kW)
P_T^{max}	The size of the transformer (kW)
Binary Variables	
$I^{Net,Buy}(\gamma,\omega,t)$	Binary variable, associated with buying power
$I^{Net,Sell}(\gamma,\omega,t)$	Binary variable, associated with selling power
I_h^{EHP}	Binary variable determining the heating operation mode of the EHP
I_c^{EHP}	Binary variable determining the cooling operation mode of the EHP
I_e^{shup}	Binary variable relating to the shift up DR
I_e^{shdo}	Binary variable relating to shift down DR
$I_{ec}(c)$	Binary variable of the candidate
$I_{EES/TES}^{ch}$	Binary variable showing the charging status of the EES/TES system
$I_{EES/TES}^{dis}$	Binary variable, showing the discharging status of the EES/TES system

1. Introduction

1.1. Motivation

Multi-carrier energy systems have been introduced to power systems as “energy hub” [1]. These energy networks not only enhance the power system reliability and stability, but also lead to

reducing the operating costs compared to the individual operation [2]. Besides, the coordinated operation of the energy hub systems and renewable energies caused energy hub systems to help to reduce emissions drastically.

An energy hub includes the generation, energy storage, and conversion assets. The generation assets of electrical energy in the hub comprise renewable energy resources (RERs) like solar photovoltaic (PV) panels and WTs, as well as microturbines (MT's), and combined heat and power (CHP) generation technology. Besides, boiler, electric heater (EH), electric heat pump (EHP), absorption chillers (ACs), and other assets, are utilized to supply electrical, cooling, and heating loads. Electrical, thermal, or cooling energy storage systems are available in hub as well. Owing to the simultaneous impacts of electrical, heating, and cooling loads and various generation and conversion assets on the energy hub operation, the planning and operation of the energy hub has faced more challenges compared to the separate electrical and gas networks.

Lack of accurate prediction of various loads of hubs and use of RERs like PV and WT cause the planning and operation of the energy hub to face many uncertainties. This issue motivates the authors of this article to consider almost all the uncertainties in the proposed model. To this end, the Monte-Carlo simulation (MCS) method would be employed to provide scenarios related to different types of loads. For the scenarios related to the uncertainties of WT power generation, historical data are used.

With the advent of DR programs in recent years, the role of end consumers in the electricity market has become much more prominent. DR programs are generally categorized into price-based and incentive-based programs. In multi-carrier energy systems, DR programs can be applied to thermal and cooling loads in addition to electrical loads, called IDR programs. It is noteworthy that by participating in these programs, consumers shift part of their load from peak hours to off-peak

hours, thereby increasing flexibility, increasing system reliability and reducing operating costs. It should be noted that the impact of DR and IDR programs on the load demand curve and costs is different. Therefore, in this study, a comprehensive study is performed on the effect of different DR and IDR programs on the results of planning and operation.

Determining the size of hub equipment in the presence of renewable resources and storage systems, and by considering short-term operating constraints as well as DR/IDR programs, is a huge problem with many decision variables. Therefore, choosing the method of solving this problem is very important. In this paper, in order to linearize the mentioned problem, a two-stage framework is presented, which solves the problems of sizing and operation in two separate stages. Besides, the effect of continuous and discrete solution space on the speed of problem solving and planning results is investigated. In this regard, the problem of optimal determination of the capacity of assets is solved in the continuous and discrete modes. Noted that the operation problem is also tackled for four seasons by considering the seasonal variation pattern in the proposed model.

1.2. Literature review

As described previously, the mentioned joint operation and planning of an energy hub would encounter severe uncertainties, mainly due to the volatile renewable power generation, and forecast error of the market price and uncertain load demand. In this regard, a bi-level mixed-inter linear programming (MILP) model was presented for the optimal planning of multi-carrier energy systems in [3] taking into consideration the impacts of distributed energy resources (DERs). The type of assets was settled in the first level while the communication between assets was specified in the second level. To improve efficiency, decrease pollution, and improve reliability, a novel framework for the optimal planning of the energy hub systems was devised in [4]. Furthermore, a

reliability and vulnerability evaluation framework has been developed in [5] for multi-energy networks by using the models of the energy hub. An innovative optimal sizing strategy was presented in [6] for a multi-carrier energy system with IDR programs. In this model, the matrix structure was deployed. The role of IDR programs in the determination of the capacity of assets was also investigated. Ref. [7] presented a standardized multi-step modeling method for the management of an energy hub. First, the primary complex model of the energy hub would be separated into multiple hubs with more straightforward models by utilizing the nodes arrangement and virtual nodes insertion techniques. Afterward, the coupling matrix relating to the resulting energy hubs is simply modeled. The final coupling matrix of each hub would be attained by the multiplication of the coupling matrix. Also, electrical energy storage (EES) systems, demand response (DR) programs, and RERs in the energy hub, are considered in the mentioned model.

The mutual impacts of energy facilities and operational parameters on the planning problem are the main challenges in energy hub planning. In [8] the effect of uncertainty of operational parameters including market price, demand, and PV output power, on the resource scheduling of the energy hub, was analyzed by utilizing a risk-oriented stochastic optimization framework. Also, a MILP model is introduced in [9] for addressing the operation problem of the energy hub. In this model, the best site, installation time, and type of assets were determined, intended to achieve the minimum investment cost. In [10], a dynamic structural sizing is presented for energy hubs with residential loads. In this model, the planning horizon was separated into sub-intervals, and the installation of the components was optimally determined in each sub-interval. In [11], a multi-objective dynamic model is introduced for hub design, in which the installation year of equipment is also considered. The problem is formulated in MILP format and the optimization goals include total cost, losses and emissions. The results show that the minimization of losses and emissions

leads to an increase in the installation capacity of PV panels and, consequently, an increase in investment costs. In addition, the results indicate that considering the IDR program leads to a reduction of about 9% in total cost.

It is necessary to investigate reliable and clean energy to promote the generation, increase the competition, and grow the economy. In order to reduce the operating costs, a hybrid stochastic-interval optimization model is presented for creating robust programming [12]. In this model, the deviation and average cost are considered in a two-objective MILP model by utilizing the weighted-sum method. Also, a robust optimization approach, considering techno-economic and environmental aspects, besides the uncertainty caused by the market price, was presented for scheduling of multi-carrier energy networks [13]. Ref [14] developed a three-level concept for planning and operation of the energy hubs. This model is handled as a MILP model. The objective of the first, the second, and the third level is the investment cost minimization, worst scenario identification, and operation cost minimization, respectively.

Many research works have been recently conducted on the use of RERs in energy hubs to prevent the increase in greenhouse gas emissions, and alleviate the concerns on global warming. The energy hub with RERs has been analyzed in [15]. In this investigation, a multi-objective model by employing the ε-constraint technique has been used to simultaneously decrease carbon emission and operation costs. Besides, using clean and renewable energies in the energy hub was explored in [16,17]. In these references, an ice storage system as an emerging storage system was introduced for promoting the energy hub's performance and efficiency. Moreover, a MILP formulation for the scheduling of an energy hub, equipped with wind and solar renewable energies is presented in [18]. The results indicated the positive effect of RERs on the energy hub's increased profit and reduced cost due to reduced power purchased from the main grid.

RERs' uncertainties lead to great challenges for the optimal operation of the energy hubs. In this relation, the optimal operation of an energy hub has been investigated in [19] while addressing the uncertainties and storage systems. It is proved that the fluctuations caused by uncertainties are neutralized by using an EES system. A robust optimization model, considering forecast errors of PV power, is presented for the energy hub planning in [20]. It is noteworthy that the storage system was employed to damp the intermittency of the solar power generation and promote the system's efficiency. The competition among energy hubs operating in the island mode has been addressed in [21] by using the Cournot model and the Nash equilibrium has been derived. The interaction between the energy hubs has been modeled by using a trasactive energy trading framework in [22] where local markets have been designed to enable the energy trading between hubs. In this respect, a virtual energy hub model plant concept has been introduced in [23] which significantly improved the performance of multi-carrier energy systems by utilizing a self-scheduling strategy.

Supplying consumers' load demand considering economic and environmental constraints is categorized into the main issues in the electric power system studies. An optimal power flow model has been devised for an energy hub network with electric vehicles (EVs) in [24]. The main purpose of this model was the total cost reduction of the system such as operation and CO2 emission costs. The EVs' uncertainties were simulated by employing a scenario-based model. The coordinated performance of EVs causes the reduction of the total cost. A risk-based scheduling model was investigated in [25]. The IDR programs, heat market, and energy scheduling are all addressed by considering RER's, electricity market, and energy storage systems. The environmental issues have been addressed in the context of energy hub management problem in [26] through a stochastic optimization problem, tackled by using the quantum particle swarm optimization (QPSO) method.

A bi-objective optimization framework has also been devised in [27], incorporating the total cost and emissions minimization as the two objective functions of the problem.

During the recent two decades, DR program implementation has been very interesting for flattening the load profile of the system and alleviating the operating costs. Accordingly, a mixed-integer non-linear programming (MINLP) model was presented for the coordinated scheduling of an energy hub with WTs and DR programs [28], taking into consideration the degradation of the energy storage systems. The role of the DR programs in the system's economic operation, reliability, and flexibility has been investigated in [29]. Moreover, the energy hub planning with DR programs, intended to alleviate the costs, has been studied in [30]. The authors in [31] present a robust optimization model for the operation of a hospital hub in which the problem is solved under both normal and emergency situations. The problem is formulated in MINLP format and its objective function is to minimize operating costs. This model is implemented on a real case study located in Hamedan, Iran and the results demonstrate that the use of robust method leads to a 6.41% increase in operating costs. The results also illustrate that the presence of storage systems leads to a reduction of about 1% in operating costs. In [32] a comprehensive analysis has been performed on demand side management aspects. In this study, not only the advantages of DR programs are discussed but also the impact of demand side management on system reliability is investigated. Ref. [33] indicates that the development of storage systems is essential to deal with the uncertainties of RERs. In this study, the applications of storage system to reduce costs and improve reliability in the presence of RERs are investigated.

In recent years, many studies have examined the technical, economic, and environmental aspects of Dynamic line rating (DLR). DLR is a philosophy related to the electric power transmission operation aiming at maximizing load without compromising safety and environmental restrictions

[34,35]. In addition, many researchers have also explored the concept of Dynamic thermal rating (DTR) [36,37]. DTR of transmission lines is related to wind speed, wind direction, ambient temperature, and so on. Ref. [38] presents an optimization method for using DR programs with the aim of reducing losses and temperature of lines. The operation problem is modeled in the form of a multi-objective optimization problem by the fuzzy method and the GA algorithm is employed to solve it. The results of this study show that lowering the temperature of the lines leads to increasing the lifetime of the lines. The authors in [39] have proposed a new method for the coordinated operation of EES systems and DR programs. This study shows that discharging EES systems during peak hours reduces costs. The results also show that the presence of EES systems increases reliability. In [40], the optimal placement of EES systems has been done with the aim of minimizing the curtailment of solar energy. The proposed model is modeled as a two-part optimization problem and the simulation results show that the optimal placement of EES systems not only prevents the curtailment of solar energy but also enhances reliability.

1.3. Research Gap and Contribution

Table 1 provides a comparison between the model proposed in this paper and recent studies. As can be seen, none of the previous studies has conducted a comprehensive study on the impact of different DR and IDR programs on determining the capacity of hub equipment. This table also indicates that none of the previous studies have examined the effect of continuous and discrete solution spaces on the speed of calculations and planning results. Therefore, in this study, integrated planning and operation of energy hub in the presence of uncertainty of electrical, heating and cooling loads, as well as the output power of WT has been done. The problem of hub planning has been solved by continuous and discrete methods and the impact of each of these methods on

the planning and operation results has been investigated. In the proposed model, emission costs are considered for three types of gas: CO_2, SO_2, and NO_2. Also, in this model, two DR programs and three IDR programs are considered and the impact of the implementation of each of these programs on the equipment capacity and operation results is investigated in detail. Given that the intended problem is a MILP problem with many decision variables and a high computational burden, the methodology used to tackle the problem is separated into two levels. First, the capacity of the equipment of the hub would be optimally specified by using the Genetic algorithm (GA), and subsequently, the resource scheduling problem of the hub would be tackled. Overall, the novelties and main points addressed in this paper are:

- Developing a stochastic model for the joint planning and operation of the energy hub
- Dividing the solution space into two stages to increase the solution speed
- Tackling the problem by using continuous and discrete methods
- Reducing planning cost by employing RCGA
- Investigating the effect of continuous and discrete methods on the hub planning
- Assessing the impacts of various DR and IDR programs on the hub planning

1.4. Organization

The contents of the paper have been categorized as follows:

The energy hub configuration, mathematical modelling and solution method are presented in Section 2. The results, obtained from simulating the studied problem are proposed in Sections 3. Lastly, Section 4 includes some final remarks.

Table 1. Comparison of the proposed model in this paper with recent studies.

Ref.	Optimization Constraints		Planning Search Space		Optimization Model		DR Programs			Storage Systems			RES	Emission	Four Seasons Load Pattern	Impact of DR on Sizing
	Planning	Operation	Discrete	Continuous	Deterministic	Stochastic	Incentive-based	Price-based	IDR	EES	TES	CES				
[41]	✓	×	✓	×	×	✓	×	×	×	✓	✓	✓	✓	✓	×	×
[42]	✓	✓	×	✓	✓	×	×	×	✓	✓	✓	×	✓	×	✓	✓
[43]	✓	×	×	✓	✓	×	×	×	×	✓	✓	✓	✓	✓	✓	×
[44]	✓	✓	✓	×	×	✓	×	×	×	✓	×	×	✓	×	×	×
[45]	✓	×	×	✓	✓	×	×	×	×	×	×	×	×	×	×	×
[46]	✓	✓	×	✓	×	✓	×	×	×	×	×	×	×	×	×	×
[47]	✓	×	×	✓	✓	×	×	×	×	×	×	×	×	×	×	×
[48]	✓	✓	×	✓	×	✓	×	×	×	✓	✓	×	✓	×	✓	×
[49]	✓	✓	✓	×	×	✓	×	×	×	✓	×	×	✓	×	×	×
[11]	✓	✓	✓	×	×	✓	×	×	✓	✓	✓	✓	✓	×	✓	✓
[10]	✓	✓	×	✓	✓	✓	×	✓	×	✓	✓	×	✓	×	×	✓
[50]	✓	✓	✓	×	×	✓	×	✓	×	✓	✓	×	✓	×	×	×
This Paper	✓	✓	✓	✓	✓	✓	✓	✓	✓	✓	✓	×	✓	✓	✓	✓

2. Model Development

2.1. Energy Hub Configuration

Candidate components for installation in the hub are depicted in Fig. 1. As can be seen, the input of the system is electricity and natural gas, while its output comprises electrical power, cooling power, and heating power. CHP is an installation candidate for power generation. It is noteworthy that the hub provides its electrical load through CHP, wind turbine and purchase from the upstream grid. Candidates for heating power generation include boilers, EH and EHP. Due to the fact that EHP is able to generate cooling power, this equipment is also among the candidates for cooling load supply. Overall, candidates for cooling power generation are AC and EHP. In addition, EES and thermal energy storage (TES) systems are also considered as storage candidates. It should be noted that some of these components may not be installed after solving the planning problem.

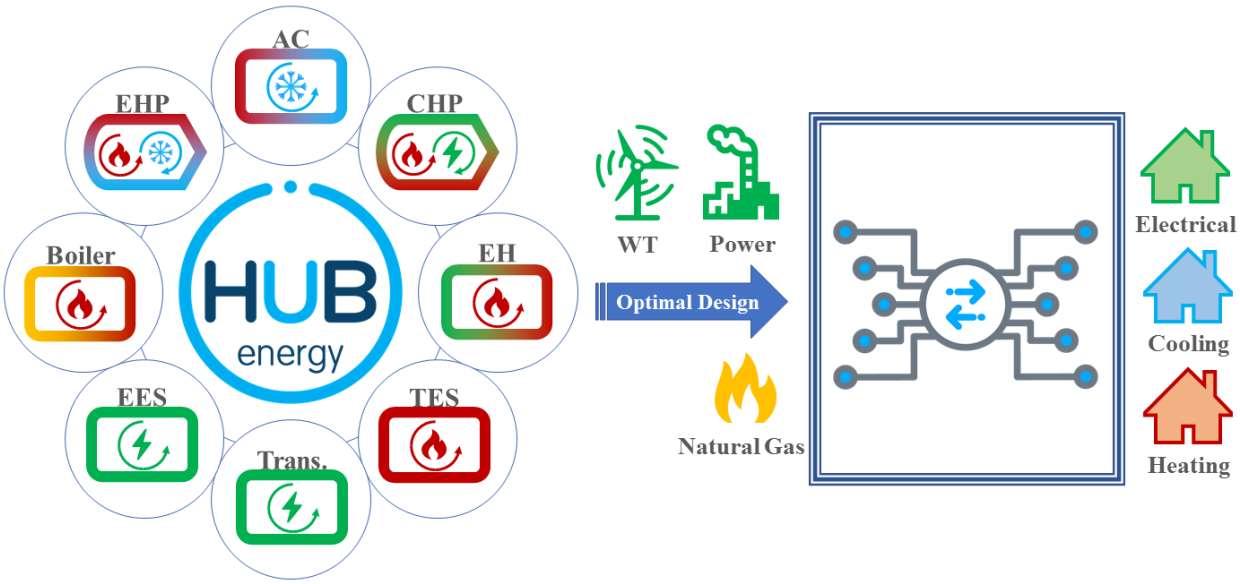

Fig. 1. The scheme of the energy hub.

2.2. Formulation

In this section, the proposed two-stage model is formulated in MILP format. In the first stage, the capacity of assets is selected, while in the second stage, the operation problem is solved. Note that

the operation problem is solved by considering seasonal variations in load and WT production. The main objective function of the model is presented in Eq. (1). As can be seen, the main objective function is to minimize total investment (IC^{Hub}) and operation (OC^{Hub}) costs.

$$Min:\ TC^{Hub} = IC^{Hub} + OC^{Hub} \tag{1}$$

2.2.1. Planning Problem Formulation

Eqs. (2)-(5) model the first stage of the proposed model. In this regard, in Eq. (2), the objective function of the first stage is presented, which is the minimization of the total investment costs. Eq. (2) shows that the total investment cost comprises the total assets' installation costs such as boiler, EH, EHP, AC, transformer, EES system, and TES system. Note that the interest rate and lifetime of assets are also considered in the objective function of investment [51]. k, r, and C_{ec} are the lifetime of assets, interest rate, and investment cost of each asset, respectively.

$$IC^{Hub} = \sum_{ec=1}^{EC} \frac{r(1+r)^k}{(1+r)^k - 1} C_{ec} \tag{2}$$

Eq. (3) calculates the investment cost of each asset according to its selected capacity. In this equation, IC_{ec} and P_{ec}^{max} are the new capacity installation cost per kilowatt, and the capacity installation of each asset in the continuous mode, respectively.

$$C_{ec} = IC_{ec} P_{ec}^{\max} \tag{3}$$

Eq. (4) is presented to solve the model in discrete space. Since the installation capacities are certain values in the discrete mode, the binary variable $I_{ec}(c)$ is used in equation (4) [52]. Finally, Eq. (5) prevents the selection of more than one candidate for each asset.

$$P_{ec}^{\max} = \sum_{c=1}^{C} P_{ec}^{Install}(c) I_{ec}(c) \tag{4}$$

$$0 \le \sum_{c=1}^{C} I_{ec}(c) \le 1 \tag{5}$$

2.2.2. Operation Problem Formulation

Eq. (6) illustrates the operating cost of the system for one year. Where $\varphi(\omega)$ and $\rho(\gamma)$ represent the number of days of a season and the probability, associated with any of the scenarios, respectively. Besides, Eq. (7) represents the cost and revenue due to transacting power with the utility grid. Eq. (8) indicates the operating cost of the CHP and boiler. Eq. (9) expresses the operating costs of the storage systems. Fuurthermore, the emission cost of CO_2, SO_2, and NO_2 has also been incorporated [53]. In this respect, the emission cost relating to the CHP unit and boiler is calculated as Eq. (10). Lastly, the cost of the DR program, and the penalty of the energy not served (ENS) are represented in Eqs. (10) and (11), respectively. It should be mentioned that Δ_t is equal to 1 hour.

$$OC^{Hub} = \sum_{sc=1}^{SC} \rho(\gamma) \sum_{s=1}^{S} \varphi(\omega) \sum_{t=1}^{T} \left[\mathrm{Cos}t^{EL} + \mathrm{Cos}t^{NG} + \mathrm{Cos}t^{ES} + \mathrm{Cos}t^{EM} + \mathrm{Cos}t^{DR} + \mathrm{Cos}t^{ENS} \right] \quad (6)$$

$$Cost^{EL} = \left(\pi_e^{Net,Buy}(\omega,t) P_e^{Net,Buy}(\gamma,\omega,t) - \pi_e^{Net,Sell}(\omega,t) P_e^{Net,Sell}(\gamma,\omega,t) \right) \Delta_t \quad (7)$$

$$Cost^{NG} = \left(\pi_g^{Net} P_g^{Net,CHP}(\gamma,\omega,t) + \pi_g^{Net} P_g^{Net,B}(\gamma,\omega,t) \right) \Delta_t \quad (8)$$

$$Cost^{ES} = \pi_e^{S} \left(P_{EES}^{ch}(\gamma,s,t) + P_{EES}^{dis}(\gamma,\omega,t) \right) \Delta_t + \pi_h^{S} \left(P_{TES}^{ch}(\gamma,\omega,t) + P_{TES}^{dis}(\gamma,\omega,t) \right) \Delta_t \quad (9)$$

$$Cost^{EM} = \sum_{em=1}^{EM} \left(\pi_{em} EF_{em}^{CHP} P_g^{Net,CHP} + \pi_{em} EF_{em}^{B} P_g^{Net,B} \right) \Delta_t \quad (10)$$

$$Cost^{DR} = \pi_k^{DR} \left(P_{e,h,c}^{+}(\gamma,\omega,t) + P_{e,h,c}^{-}(\gamma,\omega,t) \right) \Delta_t \quad (11)$$

$$Cost^{ENS} = \pi_e^{ENS} P_e^{ENS}(\gamma,\omega,t) \Delta_t \quad (12)$$

2.2.2.1. Energy Exchange Constraints

Eqs. (13) and (14) limit the purchase and sale of power from/to the grid, respectively. Constraint (15) states that the hub is not able to buy and sell power at the same time. Constraint (16) also

models the restriction of gas purchase from the network. It is noted that energy exchange for electricity is bidirectional while natural gas is unidirectional, i.e. from the main system to the hub.

$$P_e^{Net,\min} I^{Net,Buy}(\gamma,\omega,t) \le P_e^{Net,Buy}(\gamma,\omega,t) \le P_e^{Net,\max} I^{Net,Buy}(\gamma,\omega,t) \quad \forall \gamma, s, t \quad (13)$$

$$P_e^{Net,\min} I^{Net,Sell}(\gamma,\omega,t) \le P_e^{Net,Sell}(\gamma,\omega,t) \le P_e^{Net,\max} I^{Net,Sell}(\gamma,\omega,t) \quad \forall \gamma, \omega, t \quad (14)$$

$$0 \le I^{Net,Buy}(\gamma,\omega,t) + I^{Net,Sell}(\gamma,\omega,t) \le 1 \quad \forall \gamma, \omega, t \quad (15)$$

$$P_g^{Net,\min} \le P_g^{Net}(\gamma,\omega,t) \le P_g^{Net,\max} \quad \forall \gamma, \omega, t \quad (16)$$

2.2.2.2. Modelling of Storage Systems

The equations of EES and TES systems are illustrated in (17)-(24). Constraint (17) represents the stored energy rate in the storage system at every hour. The amounts of energy available in the storage system at the initial and final hours of operation are described by Eqs. (18) and (19), respectively. Eq. (20) models the loss rate at every hour. The lower and upper bounds of energy available in the storage system are shown through constraint (21). Besides, constraints (22) and (23) represent the allowable charging and discharging rates at every hour, respectively. Constraint (24) shows that the storage system can operate only in the charging or discharging modes at every hour [54].

$$E_{EES/TES}^{S}(\gamma,\omega,t) = E_{EES/TES}^{S}(\gamma,\omega,t-1) + P_{EES/TES}^{ch}(\gamma,\omega,t)\eta_{EES/TES}^{ch}\Delta_t - \frac{P_{EES/TES}^{dis}(\gamma,\omega,t)}{\eta_{EES/TES}^{dis}}\Delta_t - E_{EES/TES}^{Loss}(\gamma,\omega,t) \quad \forall \gamma, \omega, t \rangle 1 \quad (17)$$

$$E_{EES/TES}^{S}(\gamma,\omega,t) = \alpha_{EES/TES}^{Initial} P_{EES/TES}^{\max} \quad \forall \gamma, \omega, t = 0 \quad (18)$$

$$E_{EES/TES}^{S}(\gamma,\omega,t) = \alpha_{EES/TES}^{Final} P_{EES/TES}^{\max} \quad \forall \gamma, \omega, t = 24 \quad (19)$$

$$E_{EES/TES}^{Loss}(\gamma,\omega,t) = \alpha_{EES/TES}^{Loss} E_{EES/TES}^{S}(\gamma,\omega,t) \quad \forall \gamma, \omega, t \quad (20)$$

$$\alpha_{EES/TES}^{\min} P_{EES/TES}^{\max} \le E_{EES/TES}^{S}(\gamma,\omega,t) \le \alpha_{EES/TES}^{\max} P_{EES/TES}^{\max} \quad \forall \gamma, \omega, t \quad (21)$$

$$\alpha_{EES/TES}^{\min,ch} P_{EES/TES}^{\max} I_{EES/TES}^{ch} \le P_{EES/TES}^{ch}(\gamma,\omega,t) \le \alpha_{EES/TES}^{\max,ch} P_{EES/TES}^{\max} I_{EES/TES}^{ch} \quad \forall \gamma,\omega,t \quad (22)$$

$$\alpha_{EES/TES}^{\min,dis} P_{EES/TES}^{\max} I_{EES/TES}^{dis} \le P_{EES/TES}^{dis}(\gamma,\omega,t) \le \alpha_{EES/TES}^{\max,dis} P_{EES/TES}^{\max} I_{EES/TES}^{dis} \quad \forall \gamma,\omega,t \quad (23)$$

$$0 \le I_{EES/TES}^{ch}(\gamma,\omega,t) + I_{EES/TES}^{dis}(\gamma,\omega,t) \le 1 \quad \forall \gamma,\omega,t \quad (24)$$

2.2.2.3. DR and IDR Programs

In order to investigate the impact of DR and IDR programs on system flexibility and planning and operation costs, the proposed model is solved by considering different DR and IDR programs [55]. For this purpose, two traditional DR programs and three IDR programs are introduced in this section. It's worth mentioning that to measure the individual impact of each DR/IDR program, the problem was solved using one DR/IDR program in each execution.

2.2.2.3.1. Shiftable DR program

In this program, customers transfer their load to the off-peak time slots for a reward. The sum of the daily load demand remains constant, and only a part of the load would be transferred from one hour to another. Shiftable DR program's constraints were provided below.

$$\sum_{t=1}^{T} P_e^{sh,up}(\gamma,\omega,t) = \sum_{t=1}^{T} P_e^{sh,do}(\gamma,\omega,t) \quad \forall \gamma,\omega,t \quad (25)$$

$$0 \le P_e^{sh,up}(\gamma,\omega,t) \le LPF^{sh,up} P_e(\gamma,\omega,t) I_e^{sh,up}(\gamma,\omega,t) \quad \forall \gamma,\omega,t \quad (26)$$

$$0 \le P_e^{sh,do}(\gamma,\omega,t) \le LPF^{sh,do} P_e(\gamma,\omega,t) I_e^{sh,do}(\gamma,\omega,t) \quad \forall \gamma,\omega,t \quad (27)$$

$$0 \le I_e^{sh,up}(\gamma,\omega,t) + I_e^{sh,do}(\gamma,\omega,t) \le 1 \quad \forall \gamma,\omega,t \quad (28)$$

2.2.2.3.2. Price-based DR program

In the priced-based DR, customers decrease or increase their demand based on the electricity price. In this model, the demand decreases and increases depend upon the price change rate as well as demand elasticity. The model's constraints are as follows [56].

$$\sum_{t=1}^{T} P_e^{pb,up}(\gamma,\omega,t) = \sum_{t=1}^{T} P_e^{pb,do}(\gamma,\omega,t) \qquad \forall \gamma,\omega,t \qquad (29)$$

$$P_e^{pb,up}(\gamma,\omega,t) \geq \varepsilon^{up}.P_e(\gamma,\omega,t)\left(1-\frac{\pi_e^{Net}(\omega,t)}{\pi_e^{Ref}(\omega)}\right) \qquad \forall \gamma,\omega,t \qquad (30)$$

$$P_e^{pb,do}(\gamma,\omega,t) \geq \varepsilon^{do}.P_e(\gamma,\omega,t)\left(\frac{\pi_e^{Net}(\omega,t)}{\pi_e^{Ref}(\omega)}-1\right) \qquad \forall \gamma,\omega,t \qquad (31)$$

$$0 \leq P_e^{pb,up}(\gamma,\omega,t) \leq P_e(\gamma,\omega,t).B^{up}.I^{pb,up}(\gamma,\omega,t) \qquad \forall \gamma,\omega,t \qquad (32)$$

$$0 \leq P_e^{pb,do}(\gamma,\omega,t) \leq P_e(\gamma,\omega,t).B^{do}.I^{pb,do}(\gamma,\omega,t) \qquad \forall \gamma,\omega,t \qquad (33)$$

$$0 \leq I^{pb,up}(\gamma,\omega,t) + I^{pb,do}(\gamma,\omega,t) \leq 1 \qquad \forall \gamma,\omega,t \qquad (34)$$

2.2.2.3.3. Shiftable IDR

The IDR programs would enable all types of load demand to participate in the demand-side management. In other words, DR programs are employed for the three types of the load demand. The constraints of the shifting IDR mechanism simulation are provided in (35)-(38). This program's simulation method is similar to the shifting DR program, except that the program has been applied to the cooling and heating loads [57].

$$\sum_{t=1}^{T} P_{e,h,c}^{sh,up}(\gamma,\omega,t) = \sum_{t=1}^{T} P_{e,h,c}^{sh,do}(\gamma,\omega,t) \qquad \forall \gamma,\omega,t \qquad (35)$$

$$0 \leq P_{e,h,c}^{sh,up}(\gamma,\omega,t) \leq LPF^{sh,up} P_{e,h,c}(\gamma,\omega,t) I_{e,h,c}^{sh,up}(\gamma,\omega,t) \qquad \forall \gamma,\omega,t \qquad (36)$$

$$0 \leq P_{e,h,c}^{sh,do}(\gamma,\omega,t) \leq LPF^{sh,do} P_{e,h,c}(\gamma,\omega,t) I_{e,h,c}^{sh,do}(\gamma,\omega,t) \qquad \forall \gamma,\omega,t \qquad (37)$$

$$0 \leq I_{e,h,c}^{sh,up}(\gamma,\omega,t) + I_{e,h,c}^{sh,do}(\gamma,\omega,t) \leq 1 \qquad \forall \gamma,\omega,t \qquad (38)$$

2.2.2.3.4. Transferable IDR

This type of IDR program relates to the time a load starts to consume which is possible to transfer while the consumption duration should remain unchanged. Typically, it would not be possible to interrupt this type of load demand, and the amount of load demand over the day would be unchanged.

$$P_{e,h,c}^{tr,do}(\gamma,\omega,t) = P_{e,h,c}^{tr,up}(\gamma,\omega,t+N_x) \qquad \forall \gamma,\omega,t \qquad (39)$$

$$0 \le P_{e,h,c}^{tr,up}(\gamma,\omega,t) \le LPF^{tr,up} P_{e,h,c}(\gamma,\omega,t) I_{e,h,c}^{tr,up}(\gamma,\omega,t) \qquad \forall \gamma,\omega,t \qquad (40)$$

$$0 \le P_{e,h,c}^{tr,do}(\gamma,\omega,t) \le LPF^{tr,do} P_{e,h,c}(\gamma,\omega,t) I_{e,h,c}^{tr,do}(\gamma,\omega,t) \qquad \forall \gamma,\omega,t \qquad (41)$$

$$0 \le I_{e,h,c}^{tr,up}(\gamma,\omega,t) + I_{e,h,c}^{tr,do}(\gamma,\omega,t) \le 1 \qquad \forall \gamma,\omega,t \qquad (42)$$

2.2.2.3.5. Curtailable IDR

This IDR program enables the decision maker to curtail the load at a given time, but the load rebound may occur for the subsequent time intervals.

$$P_{e,h,c}^{cu,do}(\gamma,\omega,t) = \varphi_1 P_{e,h,c}^{cu,up}(\gamma,\omega,t+1) + \varphi_2 P_{e,h,c}^{cu,up}(\gamma,\omega,t+2) + \varphi_3 P_{e,h,c}^{cu,up}(\gamma,\omega,t+3) \qquad \forall \gamma,\omega,t \qquad (43)$$

$$0 \le P_{e,h,c}^{cu,up}(\gamma,\omega,t) \le LPF^{cu,up} P_{e,h,c}(\gamma,\omega,t) I_{e,h,c}^{cu,up}(\gamma,\omega,t) \qquad \forall \gamma,\omega,t \qquad (44)$$

$$0 \le P_{e,h,c}^{cu,do}(\gamma,\omega,t) \le LPF^{cu,do} P_{e,h,c}(\gamma,\omega,t) I_{e,h,c}^{cu,do}(\gamma,\omega,t) \qquad \forall \gamma,\omega,t \qquad (45)$$

2.2.2.4. Power Balance Constraints

Constraints (46)-(48) ensure the balance of production and consumption of electrical, heating and cooling powers, respectively. These constraints express that the amount of production and consumption in scenario *s* and time *t* must be equal. These constraints also indicate that storage system discharge and load reduction through the DR/IDR program are on the production side, while storage system charge and load increase through the DR/IDR program are on the consumption side.

$$
\begin{aligned}
&P_e(\gamma,\omega,t)+\frac{P_e^{Net,sell}(\gamma,\omega,t)}{\eta_{ee}^{T}}+P_{EES}^{ch}(\gamma,\omega,t)+P_e^{+}(\gamma,\omega,t)+\\
&\quad+\frac{P_h^{EHP}(\gamma,\omega,t)}{\eta_{eh}^{EHP}}+\frac{P_c^{EHP}(\gamma,\omega,t)}{\eta_{ec}^{EHP}}+P_e^{EH}(\gamma,\omega,t)\\
&\quad=\eta_{ee}^{T}P_e^{Net,Buy}(\gamma,\omega,t)+\eta_{ge}^{CHP}P_g^{Net,CHP}(\gamma,\omega,t)\\
&\quad+\eta_{ee}^{Con}P_e^{W}(\gamma,\omega,t)+P_{EES}^{dis}(\gamma,\omega,t)+P_e^{-}(\gamma,\omega,t)\\
&\quad+P_e^{ENS}(\gamma,\omega,t)
\end{aligned}
\qquad \forall\gamma,\omega,t \qquad (46)
$$

$$
\begin{aligned}
&P_h(\gamma,\omega,t)+P_{TES}^{ch}(\gamma,\omega,t)+P_h^{AC}(\gamma,\omega,t)+P_h^{+}(\gamma,\omega,t)\\
&\quad=\eta_{gh}^{CHP}P_g^{Net,CHP}(\gamma,\omega,t)+\eta_{gh}^{B}P_g^{NetB}(\gamma,\omega,t)\\
&\quad+P_{TES}^{dis}(\gamma,\omega,t)+P_h^{EHP}(\gamma,\omega,t)\\
&\quad+\eta_{eh}^{EH}P_e^{EH}(\gamma,\omega,t)+P_h^{-}(\gamma,\omega,t)
\end{aligned}
\qquad \forall\gamma,\omega,t \qquad (47)
$$

$$
P_c(\gamma,\omega,t)+P_c^{+}(\gamma,\omega,t)=\eta_{hc}^{AC}P_h^{AC}(\gamma,\omega,t)+P_c^{EHP}(\gamma,\omega,t)+P_c^{-}(\gamma,\omega,t) \qquad \forall\gamma,\omega,t \qquad (48)
$$

2.2.2.5. Operation Constraints of Hub Assets

Operation constraints of Hub assets are provided in (49)-(56) [52]. In this regard, Eq. (9) states that the rate of power exchange with the grid should be less than or equal to the capacity of the transformer. Constraints (50) and (51) state that the electricity and heat generated by the CHP unit are a function of the gas consumed and its electrical and thermal efficiencies. Constraint (52) limits the amount of heat generated by the boiler. Similarly, in constraint (53), the cooling power produced by AC is limited. Note that the AC receives its heat from CHP and boiler units. Constraints (54) and (55) limit the heat and cooling produced by EHP, respectively. I_h^{EHP} and I_c^{EHP} are binary variables that represent EHP activity in heating and cooling modes, respectively. Constraint (56) prevents simultaneous production of heat and cooling by EHP. Finally, constraint (57) states that the heat generated by EH must be less than or equal to its capacity.

$$
0\le\eta_{ee}^{T}P_e^{Net,Buy}(\gamma,\omega,t)+\frac{P_e^{Net,sell}(\gamma,\omega,t)}{\eta_{ee}^{T}}\le P_T^{\max} \qquad \forall\gamma,\omega,t \qquad (49)
$$

$$0 \le \eta_{ge}^{CHP} P_g^{Net,CHP}(\gamma,\omega,t) \le P_{CHP}^{\max} \qquad \forall \gamma,\omega,t \qquad (50)$$

$$0 \le \eta_{gh}^{CHP} P_g^{Net,CHP}(\gamma,\omega,t) \le P_{CHP}^{\max} \qquad \forall \gamma,\omega,t \qquad (51)$$

$$0 \le \eta_{gh}^{B} P_g^{Net,B}(\gamma,\omega,t) \le P_B^{\max} \qquad \forall \gamma,\omega,t \qquad (52)$$

$$0 \le \eta_{hc}^{AC} P_h^{AC}(\gamma,\omega,t) \le P_{AC}^{\max} \qquad \forall \gamma,\omega,t \qquad (53)$$

$$0 \le P_h^{EHP}(\gamma,\omega,t) \le \eta_h^{EHP} P_{EHP}^{\max} I_h^{EHP}(\gamma,\omega,t) \qquad \forall \gamma,\omega,t \qquad (54)$$

$$0 \le P_c^{EHP}(\gamma,\omega,t) \le \eta_c^{EHP} P_{EHP}^{\max} I_c^{EHP}(\gamma,\omega,t) \qquad \forall \gamma,\omega,t \qquad (55)$$

$$0 \le I_h^{EHP}(\gamma,\omega,t) + I_c^{EHP}(\gamma,\omega,t) \le 1 \qquad \forall \gamma,\omega,t \qquad (56)$$

$$0 \le \eta_{eh}^{EH} P_e^{EH}(\gamma,\omega,t) \le P_{EH}^{\max} \qquad \forall \gamma,\omega,t \qquad (57)$$

2.2.2.6. Operational Constraints of Hub Assets

To model the WT generation rate according to the wind speed, the following constraints are utilized [58]. Eq. (57) shows that if the wind speed is higher than the cut-out speed (v_{co}) or less than the cut-in speed (v_{ci}), the turbine output power will be zero. Eq. (58) also shows that if the wind speed is between the cut-in speed and the rated speed (v_r), the output power will be calculated through the corresponding function ($\frac{v(\gamma,\omega,t)-v_{ci}}{v_{r-}v_{ci}}$). Finally, Eq. (59) shows that if the wind speed is between the rated speed and the cut-out speed, the output power will be equal to the rated power of the turbine (P_r).

$$P_e^W(\gamma,\omega,t) = 0, \qquad v(\gamma,\omega,t) \langle v_{ci} \quad , \quad v(\gamma,\omega,t) \rangle v_{co} \qquad \forall \gamma,\omega,t \qquad (57)$$

$$P_e^W(\gamma,\omega,t) = P_r \qquad \frac{v(\gamma,\omega,t)-v_{ci}}{v_{r-}v_{ci}}, \qquad v_{ci} \langle v(\gamma,\omega,t) \langle v_r \qquad \forall \gamma,\omega,t \qquad (58)$$

$$P_e^W(\gamma,\omega,t) = P_r. \qquad v_r \le v(\gamma,\omega,t) \langle v_{co} \qquad \forall \gamma,\omega,t \qquad (59)$$

2.2.3. The Process of Generating and Reducing Scenarios

As stated, the scenarios related to the uncertain parameters are generated by probabilistic distribution functions. In this regard, electrical, heating and cooling load scenarios are generated by the normal distribution function [59], while WT output power scenarios are generated by the Weibull distribution function. It should be noted that 1000 scenarios are generated for each uncertain parameter. Eq. 60 presents the normal distribution function. Where, μ_x and σ_x are the mean and standard deviation, respectively; Δx_t is load prediction error. The values of μ_x and σ_x are assumed to be 0 and 0.3, respectively. Eq. 61 presents the Weibull distribution function. Where, λ and k are the scale and shape parameters, respectively [60]. The values of λ and k are assumed to be 1 and 1.5, respectively.

Since problem solving for 1000 scenarios is very time consuming, the number of initial scenarios is reduced to 10 by the ScenRed tool in GAMS software.

$$f\left(\Delta x_t;\mu_x,\sigma_x^2\right)=\frac{1}{\sqrt{2\pi\sigma_x^2}}\exp\left[-\frac{\left(\Delta x_t-\mu_x\right)^2}{2\sigma_x^2}\right] \tag{60}$$

$$f(x;\lambda,k)=\begin{cases}\frac{k}{\lambda}\left(\frac{x}{\lambda}\right)^{k-1}e^{-\left(\frac{x}{\lambda}\right)^k} & ,x\geq 0\\ 0 & ,x<0\end{cases} \tag{61}$$

2.3. Methodology

The integrated planning problem of the energy hub through the continuous and discrete methods, i.e. RCGA [61] and BCGA [62] are used to solve the problem, respectively. It is noteworthy that the major difference between RCGA and BCGA relates to the way variables are defined. In other words, the variables are determined by '0' and '1' bits in the BCGA, while the variables are determined based on real numbers in the RCGA. In fact, it depends on the type of variables. The BCGA can be applied for discrete variables, while the RCGA is more useful for continuous variables since it has the benefit of requiring less memory than BCGA. The continuous variables

are represented by floating-point numbers instead of N-bit integers. Furthermore, the RCGA is inherently faster than the BCGA because the chromosome does not have to be decoded before the evaluation of the objective function. Accordingly, the algorithm is deployed according to the flowchart shown in Fig. 2. According to the flowchart, after entering the input data, the solution algorithm is selected from RCGA and BCGA. The initial population is then generated, which in this study is considered 10 times the number of variables. In the next step, a capacity is selected for each asset and the investment cost is calculated. Next, the selected capacities are sent to GAMS and the operation problem is solved. Note that if the operation is not feasible with the selected capacities, an error is sent to MATLAB (first stage) and the capacities are re-selected. Conversely, if the operation is feasible, the problem is solved with the aim of minimizing costs and the total operating cost is sent to MATLAB. Finally, the total cost is calculated, which is the sum of the total operating cost and the total investment cost. It should be mentioned that the criterion for stopping the algorithm is not to change the solution in twenty consecutive iterations.

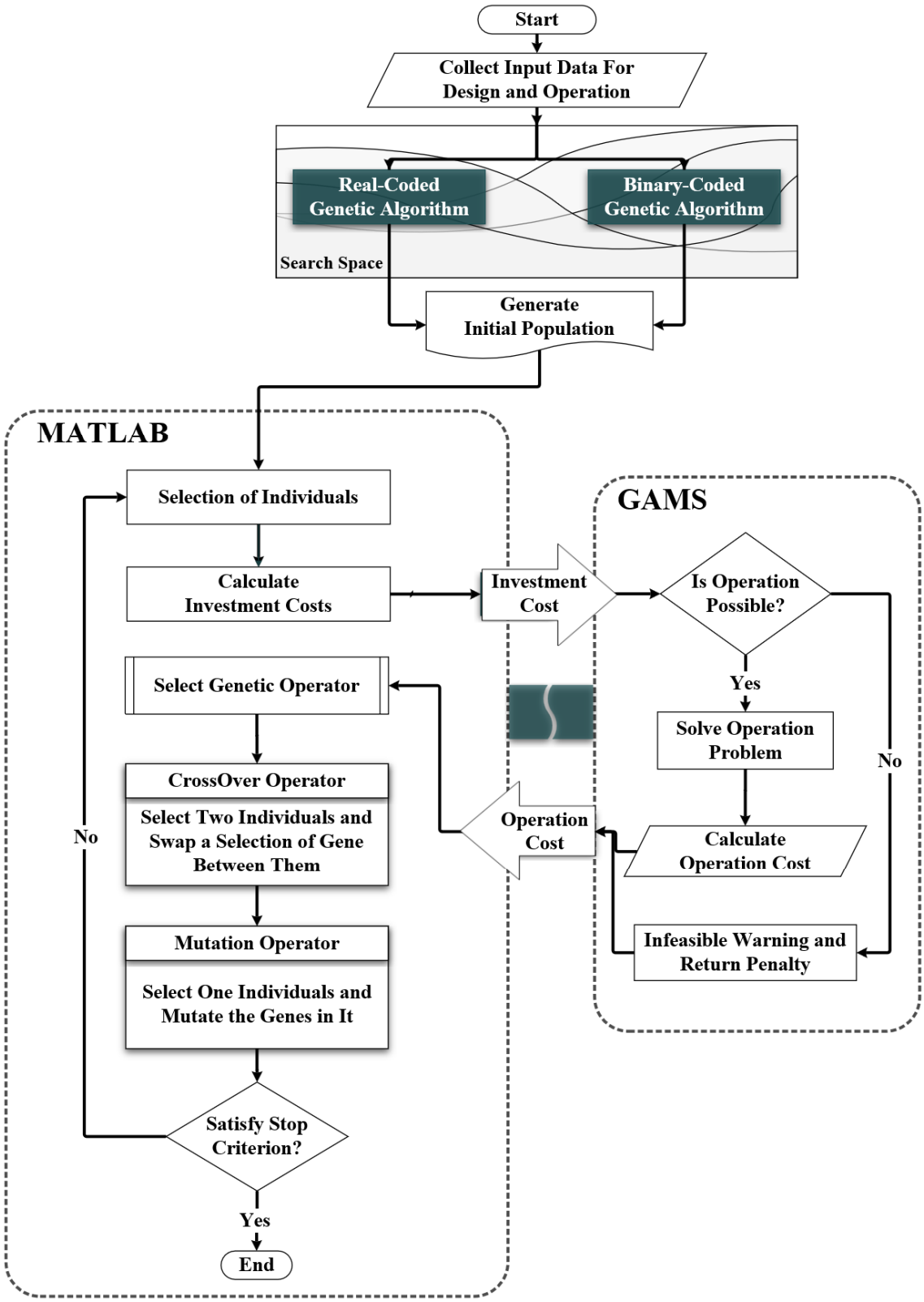

Fig. 2. The conceptual representation of the devised framework.

3. Simulation Results

3.1. Input Data

The devised problem has been tackled in the form of 10 case studies according to Table 2. As can be seen, the effect of considering the uncertainties of electrical, heating and cooling loads on the capacity of assets as well as the operating results will be fully investigated. Table 2 also illustrates that the effect of discrete and continuous solution spaces on the solution speed as well as the size of the assets will be investigated. It should be noted that in cases 1 and 6, the problem is solved deterministically without considering the uncertainties. The data of loads, as well as WT's power output, for one day of every season, are demonstrated in Fig. 3. Noted that every 24-hour period relates to one season. The peak values of the three load types and the WT's power output are respectively considered 800 kW, 600 kW, 350 kW, and 200 kW. The electricity price for each season is depicted in Fig. 4. Table 3 includes the candidate assets. Finally, the technical data of the hub assets are classified in Table 4.

Table 2. Case studies and their associated assumptions.

Case No.	Planning Mode	Uncertain Parameters			
		Wind Turbine	Electrical Load	Heating Load	Cooling Load
1	Continuous	×	×	×	×
2		✓	×	×	×
3		✓	✓	×	×
4		✓	✓	✓	×
5		✓	✓	✓	✓
6	Discrete	×	×	×	×
7		✓	×	×	×
8		✓	✓	×	×
9		✓	✓	✓	×
10		✓	✓	✓	✓

Table 3. Candidate assets in discrete mode and their installation cost [52].

Asset	Minimum Capacity (kW)	Maximum Capacity (kW)	Discrete mode's Capacity Step (kW)	Installation Cost ($/kW)

Trans.	50	500	50	450
CHP	100	500	50	990
Boiler	50	500	50	450
EH	50	300	50	400
EHP	50	300	50	500
AC	50	500	50	470
EES	50	300	50	250
TES	50	300	50	250

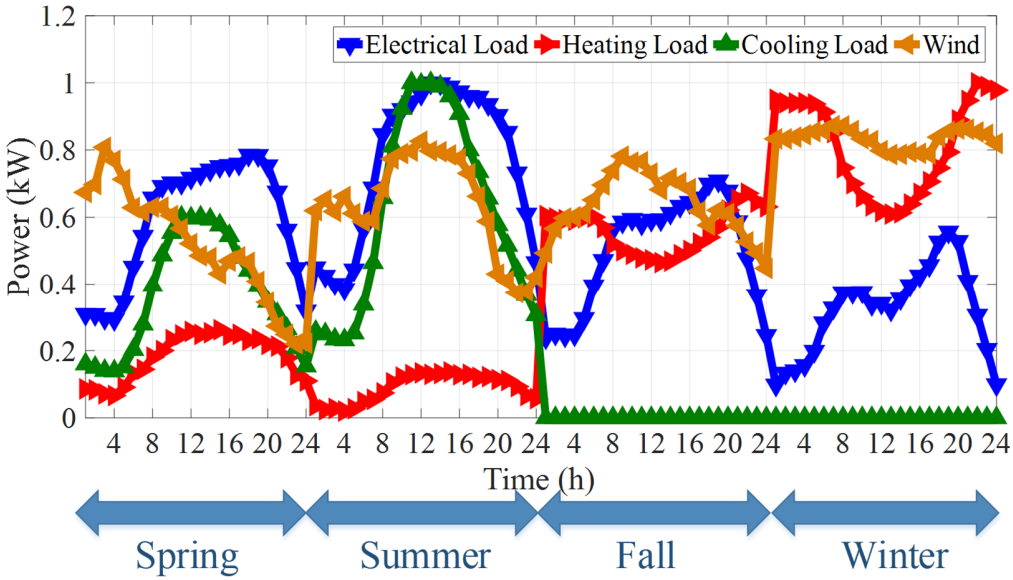

Fig. 3. The seasonal loads and wind profiles [52].

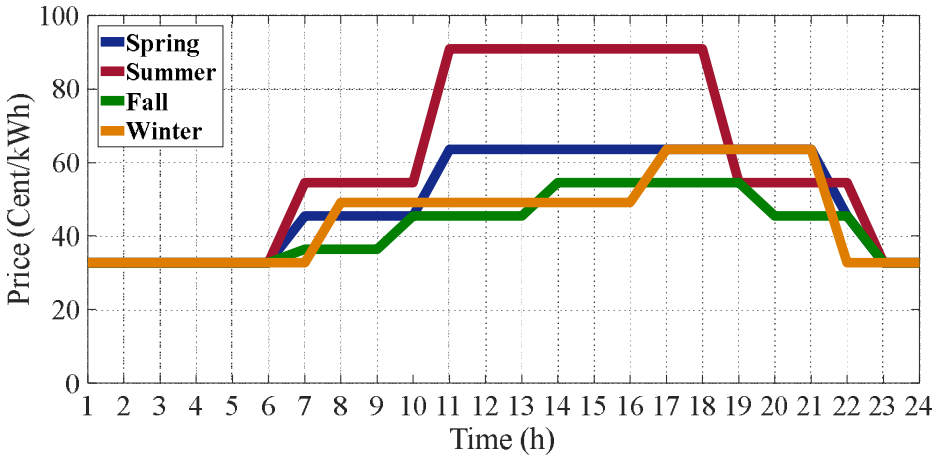

Fig. 4. The price of electrical energy [52].

Table 4. The operation data of energy hub assets [52,63].

CHP			Boiler			EES / TES		
Parameter	**Unit**	**Value**	**Parameter**	**Unit**	**Value**	**Parameter**	**Unit**	**Value**
η_{ge}^{CHP}	%	40	η_{gh}^{B}	%	85	$\eta_{EES/TES}^{ch/dis}$	%	90
η_{gh}^{CHP}	%	35	$EF_{em}^{B\,cc2}$	-	1.755	$\alpha_{EES/TES}^{Initial/final}$	%	30
$EF_{em}^{CHP\,cc2}$	-	1.596	$EF_{em}^{B\,so2}$	-	1.011	$\alpha_{EES/TES}^{min/max}$	%	10 / 90
$EF_{em}^{CHP\,so2}$	-	0.008	$EF_{em}^{B\,no2}$	-	0.62	$\alpha_{EES/TES}^{min/max,ch}$	%	0 / 25
$EF_{em}^{CHP\,no2}$	-	0.44	-	-	-	π_e^S / π_h^S	\$/kWh	0.03
Electrical Heater			**Absorption Chiller**			**Trans. and Converter**		
Parameter	**Unit**	**Value**	**Parameter**	**Unit**	**Value**	**Parameter**	**Unit**	**Value**
η_{eh}^{EH}	%	85	η_{hc}^{AC}	%	85	$\eta_{ee}^{T/Con}$	%	0.9
Wind Turbine			**DR / IDR Program**			**EHP**		
Parameter	**Unit**	**Value**	**Parameter**	**Unit**	**Value**	**Parameter**	**Unit**	**Value**
v_{ci}	m/s	4	LPF^{shdo}	%	10	η_{eh}^{EHP}	%	85
v_r	m/s	13	LPF^{shup}	%	10	η_{ec}^{EHP}	%	85
v_{co}	m/s	22	π_e^{DR}	\$/kWh	0.02	-	-	-

3.2. Continuous and Discrete Planning Results

Table 5 includes the results, derived for the studied cases. The minimum installed capacity of all assets is considered 50 kW in all cases. In the first case, the required capacity for storage systems is less than the minimum value; hence, it is set to 50 kW. The capacity of the EHP is also less than the minimum value since the installation cost of EHP is higher than the heating and cooling assets such as boiler, EH, and AC. It is therefore set to 50 kW.

In the second case, the capacity of the transformer, indicating the amount of energy bought or sold, is increased due to the uncertainty related to the WT's power generation. Also, the mentioned uncertainty causes to reduce the EH capacity and increase the capacity of the boiler, instead. Analysis of the results of Table 5 illustrates that investment and operating costs in Case 2 have

increased by 3.54% and 14.11% compared to Case 1, respectively, which is due to the choice of larger capacity for some assets and also considering the uncertainty of WT in this case.

In the third case, the electrical heater capacity is reduced again, and the transformer and EES capacity are increased. Since there is an electrical load uncertainty in addition to the wind power generation uncertainty, the capacities of the EES and generation assets of the hub are increased for facing the uncertainties. Numerical results show that considering the load uncertainties in Case 3 has led to a 0.85% increase in total cost compared to Case 2.

In the fourth case, the uncertainty related to heating load is also added to the system. In this case, the capacity of thermal assets such as boiler and CHP are increased. Besides, the capacity of TES is increased to establish the thermal equilibrium. It is noted that the transformer capacity is decreased in the fourth case due to the increased CHP capacity.

In the fifth case, the uncertainty related to the cooling load is also considered. As can be seen, the AC's capacity is increased to face cooling load uncertainty. This has been associated with the increased CHP capacity. This is due to the supplying the required thermal power of the AC by the heating power generation assets. In this case, the boiler capacity is decreased because of the increased CHP capacity. Also, the transformer's capacity is increased due to the increased EHP's capacity. Overall, the results of this section show that uncertainties have a high impact on the selected capacity of assets as well as the operation of the hub. In this regard, numerical results show that in case 5, where all uncertainties are taken into account, investment and operating costs are increased by 8.07% and 14.52% compared to case 1 (in the absence of uncertainties), respectively.

The results of continuous and discrete planning are depicted in Fig. 5. It is evident that the investment cost for the continuous planning is less than the discrete planning in all cases. However,

as shown in Fig. 6, the operation cost for discrete planning is less than the continuous one. The main reason is the higher capacity of the assets in discrete cases while buying a lower amount of power from the main electric system.

The total costs of discrete and continuous planning are compared in Fig. 7. As this figure depicts, the total costs of the hub in the continuous planning are less than the discrete one in all cases. It is noteworthy that the difference in the costs is increased by increasing the uncertainties.

Table 5. The results, derived for the continuous and discrete planning of the hub.

	Capacity (kW)									
Mode	**Continuous**					**Discrete**				
Case	**1**	**2**	**3**	**4**	**5**	**6**	**7**	**8**	**9**	**10**
AC	323.32	323.32	323.32	323.32	344.9	350	350	350	350	400
EHP	50	50	50	50	61.2	50	50	50	50	50
EH	104.8	62.68	50	53.04	50	100	50	50	100	50
Boiler	80.14	114.69	113.49	160.89	139.96	100	150	150	100	100
CHP	452.81	453.48	454.84	469.85	473.83	450	450	450	500	500
EES	50	69.54	82.97	83.26	83.52	50	100	100	100	100
TES	50	50	50	65.62	65.71	50	50	50	100	100
Trans.	291.17	349.37	380.15	316.7	331.72	300	350	350	300	350
IC ($)	171207.041	177272.76	179850.74	182407.93	185037.46	175341.82	182813.77	182813.77	190186.09	199351.69
OC($)	476861.28	544166.42	547777.33	547177.6	546122.5	473905.78	540619.58	545281.52	543875.03	541311.84
TC ($)	648068.321	721439.18	727628.07	729585.53	731159.96	649247.6	723433.35	728095.29	734061.12	740663.53

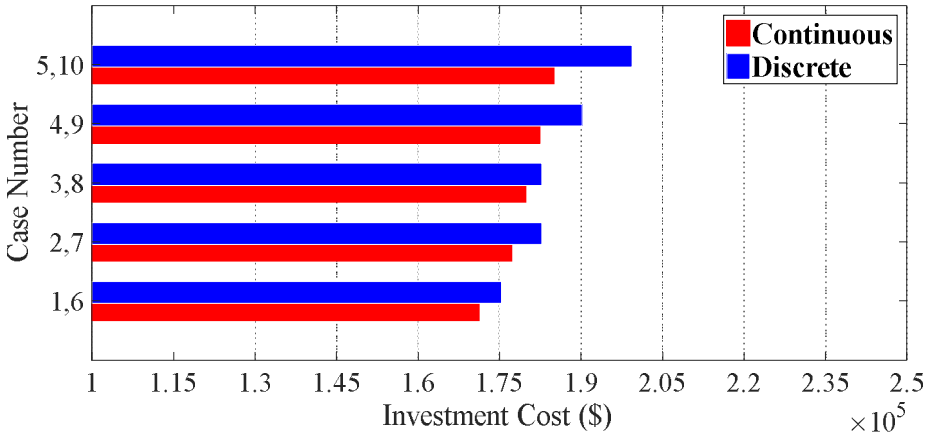

Fig. 5. The investment cost of discrete and continuous planning

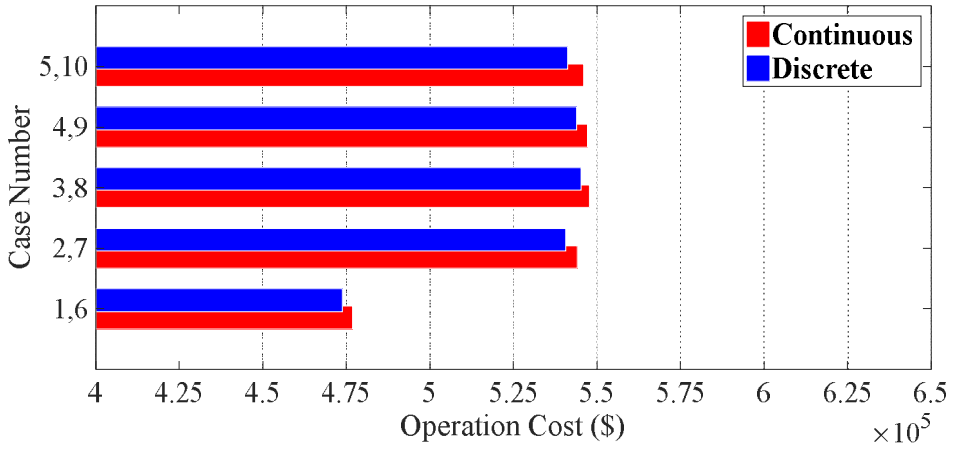

Fig. 6. The operation cost of discrete and continuous planning

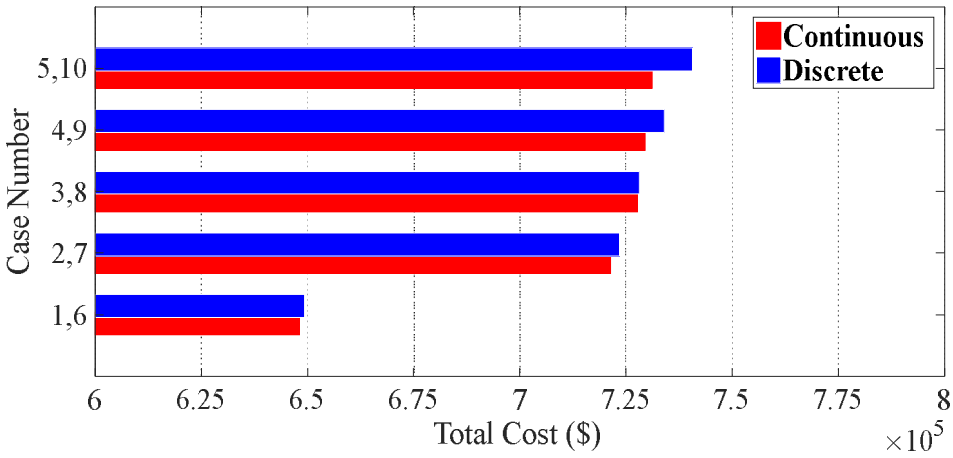

Fig. 7. The total cost of discrete and continuous planning.

3.3. Comparative Results

In this section, the operation and planning problem of the hub has been tackled by using the GAMS software and the results have been compared with the proposed model. To measure the performance and accuracy of the devised model, the results obtained through DICOPT solver are assessed with respect to the results of the proposed model, as shown in Figs. 8a and 8b. It is clear from the figures that in some cases the DICOPT solver cannot solve the problem, which these cases are marked with black squares in the figure. As Fig. 8a depicts, the total cost in the proposed

model is less than the DICOPT solver, and this difference in the discrete method (cases 6-10) is higher since the computational burden in the discrete method is higher compared to the continuous planning.

In terms of the computational burden, the execution time for different cases using DICOPT solver and the proposed model are compared in Fig. 8b. According to Fig. 8b, the execution time of the DICOPT solver is less than the proposed model since a stop at DICOPT solver occurred due to the nonconvergence in the consecutive iterations. Therefore, the obtained result does not address all planning and operation constraints. In other words, the DICOPT solver is merely able to tackle the mentioned problem in two cases.

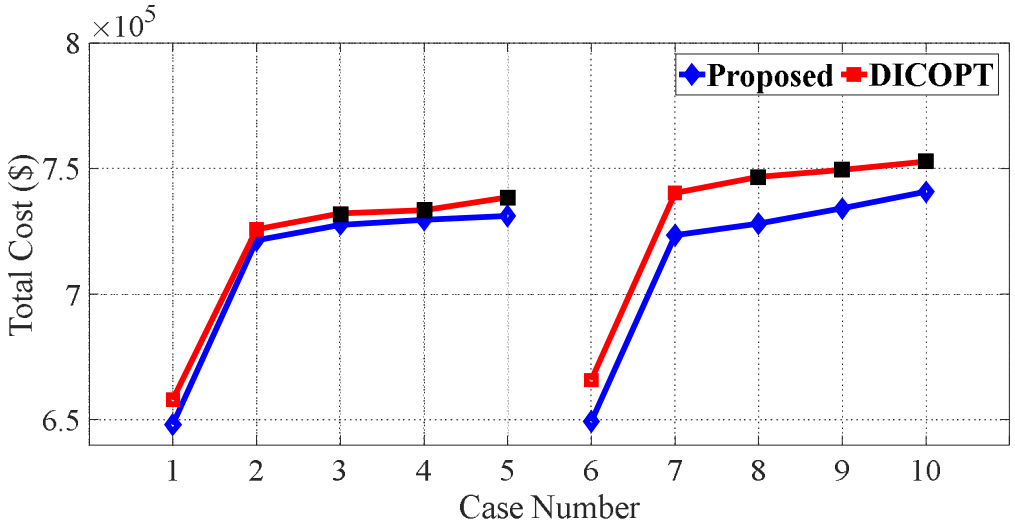

(a)

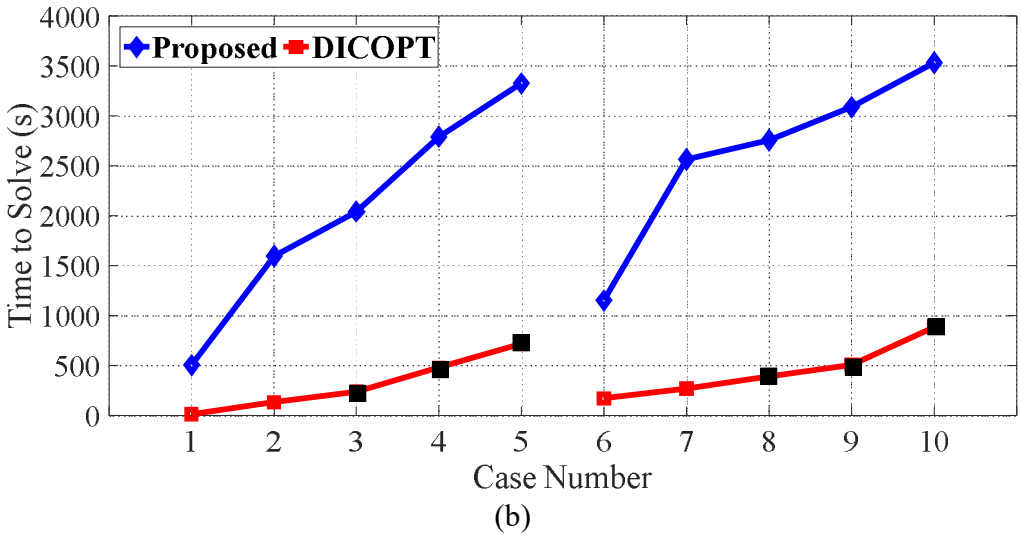

Fig. 8. (a) The comparative curves of the total cost using the DICOPT solver and proposed model, (b) execution time using the DICOPT solver, and proposed model.

3.4. The Operation Results of Case 1

The operation results of the first case are represented and discussed in this case. Besides, the 24-hour operating point of each hub asset for a typical day of every season is demonstrated in Fig. 9. As this figure indicates, the CHP unit is at its maximum operating point at all hours in winter because of the high heating load demand. Also, the boiler, EH, and EHP are contributing to the supplying heating load demand in this season. A large amount of electrical power generated in the CHP unit and WT are sold to the network to make a profit.

The assets' operating points in spring are illustrated in Fig. 9b. Since there is a cooling load demand along with the electrical and heating load demands, more equipment contribute to supplying the loads. According to Fig. 9c, the EHP and AC are responsible for supplying the cooling load in summer. The CHP unit and boiler generate the heat needed for the AC in this season. Unlike that of spring, the boiler is active in the middle of the day in addition to the early hours to supply the heat required for the AC. Fig. 9d shows the operating points of assets in fall, while the only active

assets in the generation are WT and CHP units. In this season, the electrical and heating loads are met by the CHP system, and any electrical power shortage is addressed by the WT and power purchased from the upstream grid.

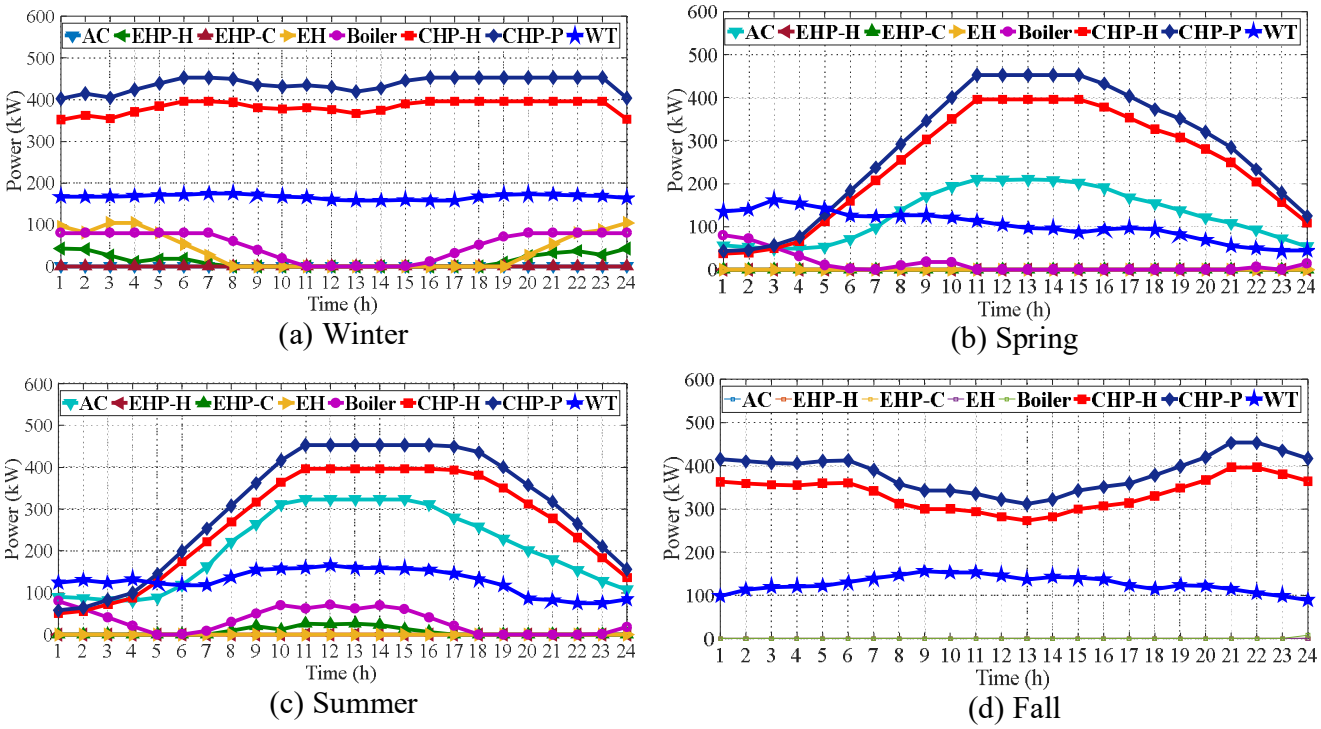

Fig. 9. The operating points of the hub assets.

In Table 6, the emission costs of the CHP and boiler units are presented for a typical day of each season. As it is obvious from this table, the maximum emission cost relates to winter, since the CHP unit is almost at its maximum operating point over the day. Also, the boiler generates more power in comparison with other seasons. The emission cost of fall is also higher than spring and summer, owing to the higher CHP generation.

The power transaction with the upstream grid is represented in Figs. 10 and 11. According to Fig. 10, the maximum power bought from the utility grid occurs in the early and late hours in spring and summer. As Fig. 11 depicts, the power sales have been at all hours in winter. Besides, the

generated power of WT and CHP is delivered to the main grid during the beginning and late time slots in fall because of the low electrical load demand. Finally, Fig. 12 shows the state of charge (SoC) of the EES system and while the SoC of the TES system is illustrated in Fig. 13.

Due to low electricity prices, the EES system absorbs power over the early time slots of the day, and delivers power to the system over the peak hours to supply the load demand, and reduce the total cost of the hub. The extra heating power generation is stored in the TES over the middle time slots of the day and then, it delivers power over the early and late hours since the heating load increases.

Table 6. Emission costs of the CHP and boiler.

Asset	Gas Type	Emission ($/day)			
		Spring	Summer	Fall	Winter
CHP	CO2	3.783	4.075	5.132	5.860
	SO2	1.341	1.444	1.819	2.077
	NO2	312.906	337.005	424.419	484.658
Boiler	CO2	0.090	0.222	0.002	0.360
	SO2	0.040	0.098	0.001	0.159
	NO2	9.585	23.514	0.261	38.117
Total		327.746	366.357	431.634	531.231

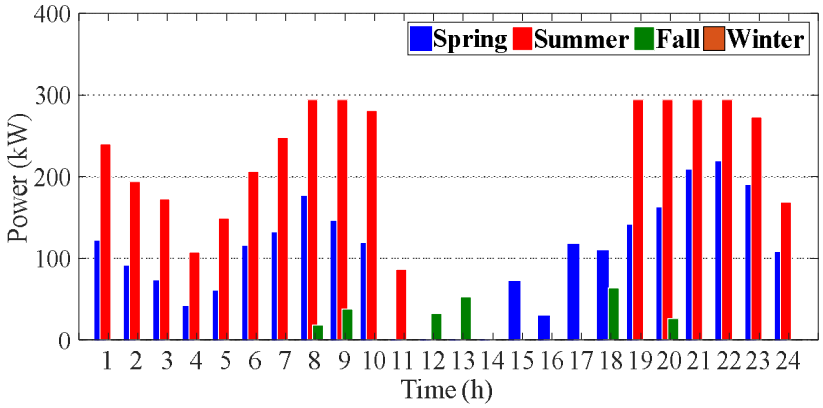

Fig. 10. Purchased power from the grid.

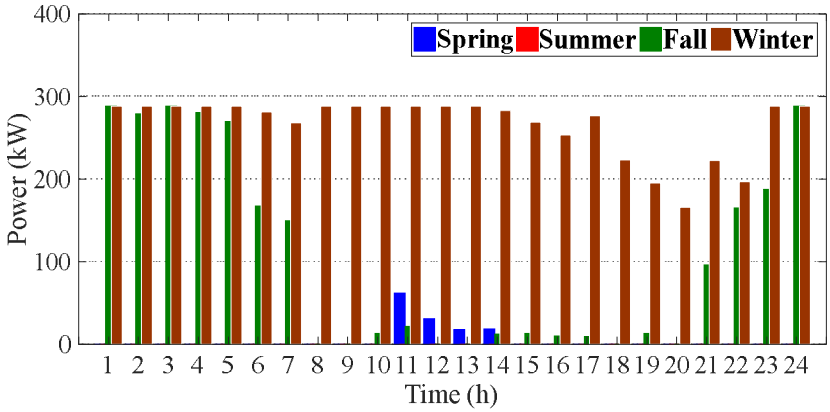

Fig. 11. Sold power to the grid.

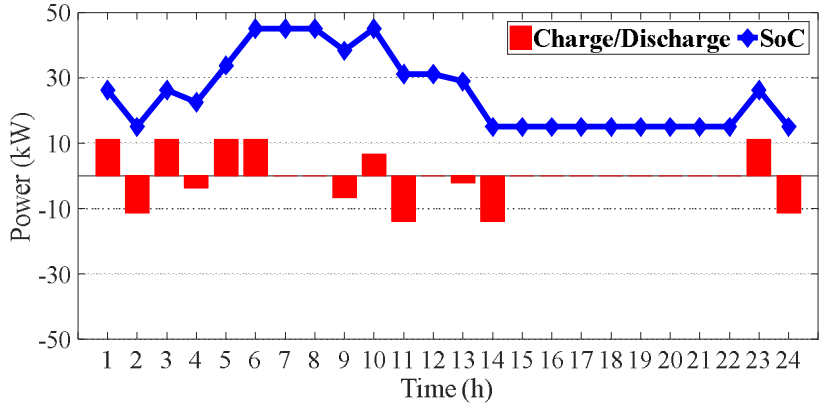

Fig. 12. SoC of EES in spring

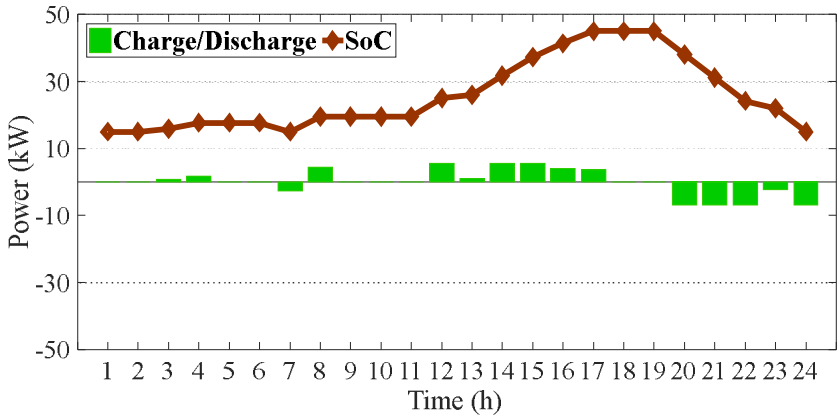

Fig. 13. SoC of TES in winter.

3.5. Assessment of DR / IDR Programs Impact

In this section, Case 5 is solved by considering different DR / IDR programs and the impact of each program on the results of planning and operation is evaluated separately. Table 7 presents the

results of solving the problem by considering each of the DR / IDR programs. Comparing the results of Table 7 with Table 5 shows that the implementation of shiftable DR program has reduced the capacity of all assets except AC, which is due to the transfer of part of the load from peak hours to non-peak hours. The results of Table 7 also illustrate that the implementation of the price-based DR program has a greater impact on reducing costs, especially operating costs, which is due to the fact that the implementation of this program is free.

In addition, a comparison of the results of different programs shows that IDR programs clearly have a much greater impact on assets capacity as well as operating costs than DR programs. Because IDR programs not only modify the demand curve of electrical load, but also the demand curve of heating and cooling loads. Numerical results illustrate that the implementation of shiftable IDR program leads to the selection of smaller capacity for assets and thus reduces investment cost by 10.26% compared to case 5. The results also indicate that the implementation of shiftable IDR program by modifying the demand curve of electrical, cooling and heating loads, has reduced operating cost by 15.1% compared to Case 5.

The impact of the shiftable IDR program on the cooling and heating demands for summer and winter are provided in Figs. (14a) and (14b), respectively. These figures show that applying the shiftable IDR program decreases the cooling load peak demand in summer, and the heating load peak in winter. Also, the shiftable IDR program effects on the electrical load demand curve of the system over the year are shown in Figs. (15a) – (15d). As can be seen, the shiftable IDR program has satisfactorily revamped the demand curve in each season by transferring the electrical load to off-peak intervals. This performance significantly increases scheduling flexibility and also improves system reliability.

Table 7. Impact of DR programs on planning and operation results.

Assets	Shiftable (DR)	Price-Based (DR)	Transferable (IDR)	Curtailable (IDR)	Shiftable (IDR)
CHP	447.55	447.94	451.55	452.16	462.76
EH	99.75	102.20	135.39	90.00	91.85
AC	351.27	349.02	313.32	322.41	290.99
EHP	50.00	50.00	50.00	50.00	50.00
Boiler	97.13	94.35	91.30	85.56	60.69
EES	50.00	50.00	50.00	50.00	50.00
TES	50.00	50.00	50.00	50.00	50.00
Trans.	283.45	280.96	265.20	271.76	276.33
IC ($/year)	173098.35	172895.45	171133.76	168560.38	166035.82
OC ($/year)	471873.45	466548.01	475797.21	478363.26	463609.84
TC ($/year)	644971.79	639443.46	646930.97	646923.64	629645.66

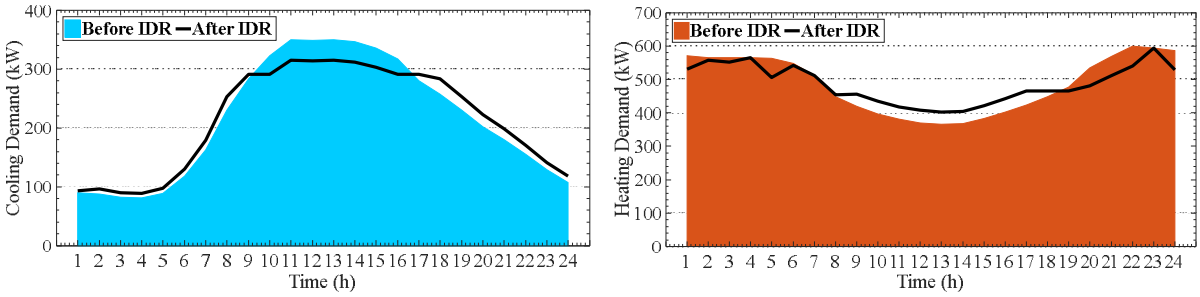

(a) The cooling demand in summer. (b) The heating demand in winter.

Fig. 14. Impact of the shiftable IDR program on the cooling and heating demand curves.

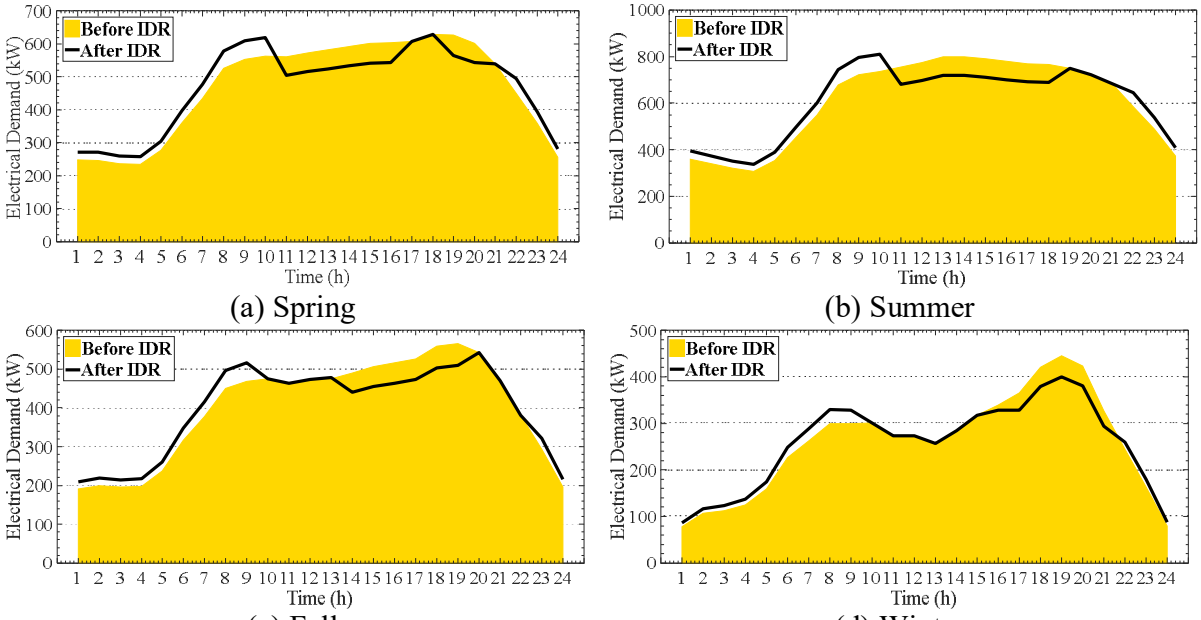

(a) Spring (b) Summer

(c) Fall (d) Winter

Fig. 15. Impact of Shiftable IDR on the electrical demand curve.

4. Conclusion

In this study a holistic framework was developed for the integrated planning and operation of an energy hub. The mentioned problem was studied for the different seasons of the year by considering uncertainties of the electrical, heating, and cooling loads as well as the WT's power output. Besides, the emission cost was considered. The proposed model was solved in the discrete and continuous modes by interfacing Matlab and GAMS software and the outstanding results obtained from this study are as follows:

- The design problem was solved by BCGA and RCGA algorithms in discrete and continuous forms, respectively, and the results demonstrated that the use of continuous method leads to more optimal results. In addition, the results illustrated that the use of continuous method leads to a reduction in solution time.
- The problem was solved by considering the uncertainties of different loads and WT output power, and the results mirrored that these uncertainties not only increased the capacity of assets but also increased the operating costs.
- Five different DR programs were applied to assess the DR programs' impact on the planning and operation results. The results show that applying the shiftable IDR program decreased the planning and operation costs, significantly, compared with other programs.
- A comparison of the proposed model with DICOPT solver in the GAMS software was substantiated that the proposed method was more precise and effective to tackle the problems with various uncertainties and heavy computational burden since the DICOPT solver is not able to solve such problems.

References

[1] Geidl M, Koeppel G, Favre-Perrod P, Klöckl B, Andersson G, Fröhlich K. Energy hubs for the future. IEEE Power Energy Mag 2007;5:24–30. https://doi.org/10.1109/MPAE.2007.264850.

[2] Fang J. Dynamic Optimal Energy Flow in the Integrated Natural Gas and Electrical Power Systems. 2018 IEEE Power Energy Soc. Gen. Meet., 2018, p. 1–1. https://doi.org/10.1109/pesgm.2018.8586246.

[3] Huang W, Zhang N, Yang J, Wang Y, Kang C. Optimal Configuration Planning of Multi-Energy Systems Considering Distributed Renewable Energy. 2019 IEEE Power Energy Soc. Gen. Meet., 2020, p. 1–1. https://doi.org/10.1109/pesgm40551.2019.8973885.

[4] Zhang X, Shahidehpour M, Alabdulwahab A, Abusorrah A. Optimal Expansion Planning of Energy Hub with Multiple Energy Infrastructures. IEEE Trans Smart Grid 2015;6:2302–11. https://doi.org/10.1109/TSG.2015.2390640.

[5] Huang W, Du E, Capuder T, Zhang X, Zhang N, Strbac G, et al. Reliability and Vulnerability Assessment of Multi-Energy Systems: An Energy Hub Based Method. IEEE Trans Power Syst 2021:1. https://doi.org/10.1109/TPWRS.2021.3057724.

[6] Qiu Z, Wang B, Huang J, Xie Z. Optimal configuration and sizing of regional energy service company's energy hub with integrated demand response. IEEJ Trans Electr Electron Eng 2019;14:383–93. https://doi.org/10.1002/tee.22819.

[7] Liu T, Zhang D, Wang S, Wu T. Standardized modelling and economic optimization of multi-carrier energy systems considering energy storage and demand response. Energy Convers Manag 2019;182:126–42. https://doi.org/10.1016/j.enconman.2018.12.073.

[8] Jadidbonab M, Dolatabadi A, Mohammadi-Ivatloo B, Abapour M, Asadi S. Risk-constrained energy management of PV integrated smart energy hub in the presence of demand response program and compressed air energy storage. IET Renew Power Gener 2019;13:998–1008. https://doi.org/10.1049/iet-rpg.2018.6018.

[9] Ghasemi H, Aghaei J, Gharehpetian GB, Safdarian A. MILP model for integrated expansion planning of multi-carrier active energy systems. IET Gener Transm Distrib 2019;13:1177–89. https://doi.org/10.1049/iet-gtd.2018.6328.

[10] Senemar S, Rastegar M, Dabbaghjamanesh M, Hatziargyriou N. Dynamic Structural Sizing of Residential Energy Hubs. IEEE Trans Sustain Energy 2020;11:1236–46. https://doi.org/10.1109/TSTE.2019.2921110.

[11] Ahmarinejad A. A Multi-objective Optimization Framework for Dynamic Planning of Energy Hub Considering Integrated Demand Response Program. Sustain Cities Soc 2021;74:103136. https://doi.org/https://doi.org/10.1016/j.scs.2021.103136.

[12] Jamalzadeh F, Hajiseyed Mirzahosseini A, Faghihi F, Panahi M. Optimal operation of energy hub system using hybrid stochastic-interval optimization approach. Sustain Cities Soc 2020;54:101998. https://doi.org/10.1016/j.scs.2019.101998.

[13] Najafi-Ghalelou A, Nojavan S, Zare K, Mohammadi-Ivatloo B. Robust scheduling of thermal, cooling and electrical hub energy system under market price uncertainty. Appl Therm Eng 2019;149:862–80. https://doi.org/10.1016/j.applthermaleng.2018.12.108.

[14] Karamdel S, Moghaddam MP. Robust expansion co-planning of electricity and natural gas infrastructures for multi energy-hub systems with high penetration of renewable energy sources. IET Renew Power Gener 2019;13:2287–97. https://doi.org/10.1049/iet-rpg.2018.6005.

[15] Cao Y, Wang Q, Du J, Nojavan S, Jermsittiparsert K, Ghadimi N. Optimal operation of CCHP and renewable generation-based energy hub considering environmental perspective: An epsilon constraint and fuzzy methods. Sustain Energy, Grids Networks 2019;20:100274. https://doi.org/10.1016/j.segan.2019.100274.

[16] Heidari A, Mortazavi SS, Bansal RC. Stochastic effects of ice storage on improvement of an energy hub optimal operation including demand response and renewable energies. Appl Energy 2020;261:114393. https://doi.org/10.1016/j.apenergy.2019.114393.

[17] Bahmani R, Karimi H, Jadid S. Cooperative energy management of multi-energy hub systems considering demand response programs and ice storage. Int J Electr Power Energy Syst 2021;130:106904. https://doi.org/https://doi.org/10.1016/j.ijepes.2021.106904.

[18] Rakipour D, Barati H. Probabilistic optimization in operation of energy hub with participation of renewable energy resources and demand response. Energy 2019;173:384–99. https://doi.org/10.1016/j.energy.2019.02.021.

[19] Javadi MS, Anvari-Moghaddam A, Guerrero JM, Esmaeel Nezhad A, Lotfi M, Catalão JPS. Optimal Operation of an Energy Hub in the Presence of Uncertainties. Proc - 2019 IEEE Int Conf Environ Electr Eng 2019 IEEE Ind Commer Power Syst Eur EEEIC/I CPS Eur 2019 2019:1–4. https://doi.org/10.1109/EEEIC.2019.8783452.

[20] Zhao P, Gu C, Huo D, Shen Y, Hernando-Gil I. Two-Stage Distributionally Robust Optimization for Energy Hub Systems. IEEE Trans Ind Informatics 2020;16:3460–9. https://doi.org/10.1109/TII.2019.2938444.

[21] Rahmatian MR, Shamim AG, Bahramara S. Optimal operation of the energy hubs in the islanded multi-carrier energy system using Cournot model. Appl Therm Eng 2021;191:116837. https://doi.org/https://doi.org/10.1016/j.applthermaleng.2021.116837.

[22] Khorasany M, Najafi-Ghalelou A, Razzaghi R, Mohammadi-Ivatloo B. Transactive energy framework for optimal energy management of multi-carrier energy hubs under local electrical, thermal, and cooling market constraints. Int J Electr Power Energy Syst 2021;129:106803. https://doi.org/https://doi.org/10.1016/j.ijepes.2021.106803.

[23] Jadidbonab M, Mohammadi-Ivatloo B, Marzband M, Siano P. Short-Term Self-Scheduling of Virtual Energy Hub Plant Within Thermal Energy Market. IEEE Trans Ind Electron 2021;68:3124–36. https://doi.org/10.1109/TIE.2020.2978707.

[24] Lu X, Liu Z, Ma L, Wang L, Zhou K, Feng N. A robust optimization approach for optimal load dispatch of community energy hub. Appl Energy 2020;259:114195.

https://doi.org/10.1016/j.apenergy.2019.114195.

[25] Tian MW, Ebadi AG, Jermsittiparsert K, Kadyrov M, Ponomarev A, Javanshir N, et al. Risk-based stochastic scheduling of energy hub system in the presence of heating network and thermal energy management. Appl Therm Eng 2019;159:113825. https://doi.org/10.1016/j.applthermaleng.2019.113825.

[26] Shahrabi E, Hakimi SM, Hasankhani A, Derakhshan G, Abdi B. Developing optimal energy management of energy hub in the presence of stochastic renewable energy resources. Sustain Energy, Grids Networks 2021;26:100428. https://doi.org/https://doi.org/10.1016/j.segan.2020.100428.

[27] Monemi Bidgoli M, Karimi H, Jadid S, Anvari-Moghaddam A. Stochastic electrical and thermal energy management of energy hubs integrated with demand response programs and renewable energy: A prioritized multi-objective framework. Electr Power Syst Res 2021;196:107183. https://doi.org/https://doi.org/10.1016/j.epsr.2021.107183.

[28] Li Y, Wang J, Han Y, Zhao Q. Generalized Modeling and Coordinated Management of Energy Hub Incorporating Wind Power and Demand Response. Proc. 31st Chinese Control Decis. Conf. CCDC 2019, 2019, p. 4214–9. https://doi.org/10.1109/CCDC.2019.8832489.

[29] Papadimitriou CN, Anastasiadis A, Psomopoulos CS, Vokas G. Demand response schemes in energy hubs: A comparison study. Energy Procedia 2019;157:939–44. https://doi.org/10.1016/j.egypro.2018.11.260.

[30] Gao Y, Xue Y, Wen F, Wang K, Huang Y, Xue Y. Planning of Energy Hubs with Demand Side Management in Integrated Electricity-Gas Energy Systems. Int. Conf. Innov. Smart Grid Technol. ISGT Asia 2018, 2018, p. 282–7. https://doi.org/10.1109/ISGT-Asia.2018.8467829.

[31] Honarmand HA, Shamim AG, Meyar-Naimi H. A robust optimization framework for energy hub operation considering different time resolutions: A real case study. Sustain Energy, Grids Networks 2021:100526. https://doi.org/https://doi.org/10.1016/j.segan.2021.100526.

[32] Jabir HJ, Teh J, Ishak D, Abunima H. Impacts of Demand-Side Management on Electrical Power Systems: A Review. Energies 2018;11. https://doi.org/10.3390/en11051050.

[33] Mohamad F, Teh J, Lai C-M, Chen L-R. Development of Energy Storage Systems for Power Network Reliability: A Review. Energies 2018;11. https://doi.org/10.3390/en11092278.

[34] Teh J. Uncertainty Analysis of Transmission Line End-of-Life Failure Model for Bulk Electric System Reliability Studies. IEEE Trans Reliab 2018;67:1261–8. https://doi.org/10.1109/TR.2018.2837114.

[35] Teh J, Lai C-M. Reliability impacts of the dynamic thermal rating and battery energy storage systems on wind-integrated power networks. Sustain Energy, Grids Networks 2019;20:100268. https://doi.org/https://doi.org/10.1016/j.segan.2019.100268.

[36] Teh J, Lai C-M, Cheng Y-H. Impact of the Real-Time Thermal Loading on the Bulk

Electric System Reliability. IEEE Trans Reliab 2017;66:1110–9. https://doi.org/10.1109/TR.2017.2740158.

[37] Lai C-M, Teh J. Network topology optimisation based on dynamic thermal rating and battery storage systems for improved wind penetration and reliability. Appl Energy 2022;305:117837. https://doi.org/https://doi.org/10.1016/j.apenergy.2021.117837.

[38] Khoo WC, Teh J, Lai C-M. Demand Response and Dynamic Line Ratings for Optimum Power Network Reliability and Ageing. IEEE Access 2020;8:175319–28. https://doi.org/10.1109/ACCESS.2020.3026049.

[39] Metwaly MK, Teh J. Probabilistic Peak Demand Matching by Battery Energy Storage Alongside Dynamic Thermal Ratings and Demand Response for Enhanced Network Reliability. IEEE Access 2020;8:181547–59. https://doi.org/10.1109/ACCESS.2020.3024846.

[40] Mohamad F, Teh J, Lai C-M. Optimum allocation of battery energy storage systems for power grid enhanced with solar energy. Energy 2021;223:120105. https://doi.org/https://doi.org/10.1016/j.energy.2021.120105.

[41] Huang W, Zhang N, Kang C, Capuder T, Holjevac N, Kuzle I. Beijing subsidiary administrative center multi-energy systems: An optimal configuration planning. Electr Power Syst Res 2020;179:106082. https://doi.org/10.1016/j.epsr.2019.106082.

[42] Zhu X, Zhou M, Xiang Z, Zhang L, Sun Y, Li G. Research on optimal configuration of energy hub considering system flexibility. In: Xue Y, Zheng Y, Rahman S, editors. Lect. Notes Electr. Eng., vol. 585, Singapore: Springer Singapore; 2020, p. 243–57. https://doi.org/10.1007/978-981-13-9783-7_19.

[43] Cheng Y, Zhang N, Kirschen DS, Huang W, Kang C. Planning multiple energy systems for low-carbon districts with high penetration of renewable energy: An empirical study in China. Appl Energy 2020;261:114390. https://doi.org/10.1016/j.apenergy.2019.114390.

[44] Roustaei M, Niknam T, Salari S, Chabok H, Sheikh M, Kavousi-Fard A, et al. A scenario-based approach for the design of Smart Energy and Water Hub. Energy 2020;195:116931. https://doi.org/10.1016/j.energy.2020.116931.

[45] Zhang H, Cao Q, Gao H, Wang P, Zhang W, Yousefi N. Optimum design of a multi-form energy hub by applying particle swarm optimization. J Clean Prod 2020;260:121079. https://doi.org/10.1016/j.jclepro.2020.121079.

[46] Amiri S, Honarvar M, sadegheih A. Providing an integrated Model for Planning and Scheduling Energy Hubs and preventive maintenance. Energy 2018;163:1093–114. https://doi.org/10.1016/j.energy.2018.08.046.

[47] Amiri K, Niknam T. Optimal Planning of a Multi-carrier Energy Hub Using the Modified Bird Mating Optimizer. Iran J Sci Technol - Trans Electr Eng 2019;43:517–26. https://doi.org/10.1007/s40998-018-0138-5.

[48] Cao Y, Wei W, Wang J, Mei S, Shafie-Khah M, Catalão JPS. Capacity Planning of Energy Hub in Multi-Carrier Energy Networks: A Data-Driven Robust Stochastic Programming Approach. IEEE Trans Sustain Energy 2020;11:3–14.

https://doi.org/10.1109/TSTE.2018.2878230.

[49] Chen C, Shen X, Guo Q, Sun H. Robust planning-operation co-optimization of energy hub considering precise model of batteries' economic efficiency. Energy Procedia 2019;158:6496–501. https://doi.org/10.1016/j.egypro.2019.01.111.

[50] Chen C, Sun H, Shen X, Guo Y, Guo Q, Xia T. Two-stage robust planning-operation co-optimization of energy hub considering precise energy storage economic model. Appl Energy 2019;252:113372. https://doi.org/10.1016/j.apenergy.2019.113372.

[51] Mansouri SA, Ahmarinejad A, Nematbakhsh E, Javadi MS, Jordehi AR, Catalão JPS. Energy Hub Design in the Presence of P2G System Considering the Variable Efficiencies of Gas-Fired Converters. 2021 Int. Conf. Smart Energy Syst. Technol., 2021, p. 1–6. https://doi.org/10.1109/SEST50973.2021.9543179.

[52] Mansouri SA, Ahmarinejad A, Ansarian M, Javadi MS, Catalao JPS. Stochastic planning and operation of energy hubs considering demand response programs using Benders decomposition approach. Int J Electr Power Energy Syst 2020;120:106030. https://doi.org/10.1016/j.ijepes.2020.106030.

[53] Pazouki S, Haghifam MR, Moser A. Uncertainty modeling in optimal operation of energy hub in presence of wind, storage and demand response. Int J Electr Power Energy Syst 2014;61:335–45. https://doi.org/10.1016/j.ijepes.2014.03.038.

[54] Mansouri SA, Ahmarinejad A, Nematbakhsh E, Javadi MS, Jordehi AR, Catalão JPS. Energy Management in Microgrids including Smart Homes: A Multi-objective Approach. Sustain Cities Soc 2021:102852. https://doi.org/https://doi.org/10.1016/j.scs.2021.102852.

[55] Mansouri SA, Ahmarinejad A, Javadi MS, Nezhad AE, Shafie-Khah M, Catalão JPS. Chapter 9 - Demand response role for enhancing the flexibility of local energy systems. In: Graditi G, Di Somma MBT-DER in LIES, editors., Elsevier; 2021, p. 279–313. https://doi.org/https://doi.org/10.1016/B978-0-12-823899-8.00011-X.

[56] Amir Mansouri S, Javadi MS, Ahmarinejad A, Nematbakhsh E, Zare A, Catalão JPS. A coordinated energy management framework for industrial, residential and commercial energy hubs considering demand response programs. Sustain Energy Technol Assessments 2021;47:101376. https://doi.org/10.1016/j.seta.2021.101376.

[57] Wang B, Yang X, Short T, Yang S. Chance constrained unit commitment considering comprehensive modelling of demand response resources. IET Renew Power Gener 2017;11:490–500. https://doi.org/10.1049/iet-rpg.2016.0397.

[58] Mansouri SA, Nematbakhsh E, Javadi MS, Jordehi AR, Shafie-khah M, Catalão JPS. Resilience Enhancement via Automatic Switching considering Direct Load Control Program and Energy Storage Systems. 2021 IEEE Int. Conf. Environ. Electr. Eng. 2021 IEEE Ind. Commer. Power Syst. Eur. (EEEIC / I&CPS Eur., 2021, p. 1–6. https://doi.org/10.1109/EEEIC/ICPSEurope51590.2021.9584609.

[59] Mansouri SA, Ahmarinejad A, Javadi MS, Catalão JPS. Two-stage stochastic framework for energy hubs planning considering demand response programs. Energy 2020;206:118124. https://doi.org/10.1016/j.energy.2020.118124.

[60] Wan J, Zheng F, Luan H, Tian Y, Li L, Ma Z, et al. Assessment of wind energy resources in the urat area using optimized weibull distribution. Sustain Energy Technol Assessments 2021;47:101351. https://doi.org/https://doi.org/10.1016/j.seta.2021.101351.

[61] Wang J, Zhang M, Ersoy OK, Sun K, Bi Y. An Improved Real-Coded Genetic Algorithm Using the Heuristical Normal Distribution and Direction-Based Crossover. Comput Intell Neurosci 2019;2019:4243853. https://doi.org/10.1155/2019/4243853.

[62] Bisht D. Comparative Analysis of Real and Binary Coded Genetic Algorithm for Fuzzy Time Series Prediction Fuzzy time series View project 2013;3:299–304.

[63] Pazouki S, Haghifam MR. Optimal planning and scheduling of energy hub in presence of wind, storage and demand response under uncertainty. Int J Electr Power Energy Syst 2016;80:219–39. https://doi.org/10.1016/j.ijepes.2016.01.044.